BIOLOGICAL EFFECT OF TYPE I PROCOLLAGEN CARBOXYTERMINAL PROPEPTIDE IN BREAST CANCER TUMOR MICROENVIRONMENT

MIGUEL FILIPE PORTUGAL DO CANTO E COSTA

A dissertation submitted in partial fulfilment of the requirements for the Degree of Masters in Biomedical Research (Specialization Area: Oncobiology) at Faculdade de Ciências Médicas | NOVA Medical School of NOVA University Lisbon

June, 2022

BIOLOGICAL EFFECT OF TYPE I PROCOLLAGEN CARBOXYTERMINAL PROPEPTIDE IN BREAST CANCER TUMOR MICROENVIRONMENT

Miguel Filipe Portugal do Canto e Costa
Supervisor: Ana Cavaco, Postdoctoral Researcher at Instituto de Medicina Molecular (iMM)
Internal advisor: Duarte Barral, Associate Professor at NOVA Medical School

A dissertation submitted in partial fulfilment of the requirements for the Degree of Masters in Biomedical Research (Specialization Area: Oncobiology)

June, 2022

Acknowledgements

One of the most important periods of my academic life has now come to an end, and despite all the setbacks and hurdles I can confidently say that I feel proud of the work I have achieved as well as immense personal growth. None of this would have been possible without the presence and unconditional support of many friends, family, and colleagues.

Firstly, I would like to thank my advisor Dra. Ana Cavaco, whom without this project would have been much more difficult and complex. For all the dedication, promptitude to help and guidance throughout this experience. But also, for all the conversations, good humor, and important tips for the future. I could not have hoped for a better mentor and friend. To Professor Luís Costa for accepting me in the lab and allowing me to develop this project and to the other elements in the lab namely, Dr. Marta Martins and Dr. Sandra Casimiro, the amazing phD students, Inês and Raquel, and the oncodynamics crew, Patricia Alves, and Patricia Corredeira, for the warm welcome, the spirit of companionship and for always being available to help. A special thanks to Sara, with whom I shared all my frustrations, my lab partner for life and to Leonor and Filipa, my zebrafish companions, for your friendship and motivation. To the fish facility of iMM, amazingly represented by Lara Carvalho and Aida Barros, for all your commitment, enthusiasm, and kindness.

To my mom, for the unconditional support and endless love, for the sacrifices made every day to assure me and my sister everything we need to be happy and succeed. To my little sister, that pushes me every day to be a better person and role model, for making my life much crazier and happier. To Sara, my dearest friend and confident, her never ending ambition and aspirations drive me to keep pursuing a better future for myself, and although we spent the majority of this year apart, we always found ways to be present in each other's lives and for that I will always be thankful. To my colleagues and friends from the NBR master programme for all the funny moments we spent together and for the solidarity shown in celebrating each other's victories. To Jéssica, for her strength, determination, and resilience that keep inspiring me every day to conquer my own achievements.

Finally, to my dad, who will always stay in my heart, I hope I am making you proud.

Abstract

Collagen is the most abundant component of the extracellular matrix, having a central role in regulating cell behavior, tissue development and providing tensile strength. In the tumor microenvironment, collagen is stiffer than in normal stroma due to increased linearization and crosslinking and increased collagen expression and density is correlated with a worse prognosis.

Desmoplasia, a process characteristic of several types of cancer, including breast carcinoma, results in enhanced type I collagen deposition. Production of type I collagen releases P1CP, a well-described robust and sensitive marker for osteoblastic activity in bone metastasis with relevant prognostic value in this disease. However, the bioactive properties of this fragment, regarding tumor progression, have been poorly explored and may represent an area of therapeutic development. Accordingly, this work aimed to explore the biological role of P1CP in breast cancer cell invasion and metastasis formation, as well as its interaction with the innate immune system using *in vitro* 3D spheroid models and *in vivo* zebrafish xenograft models.

In the *in vitro* 3D spheroid models of breast cancer cells co-cultured with monocytic cells or derived macrophages, treatment with P1CP led to an overall increase in invasive ability of cancer cells, except when in the presence of M2-like pro-tumoral macrophages. Significant increases of cancer cell invasion in the presence of THP-I, M0-, and M1-like macrophages hint a possible role of P1CP in the modulation of monocyte differentiation and macrophage polarization towards pro-tumoral phenotypes. Experiments conducted in zebrafish xenografts, hint at P1CP as a possible agent in tumor immune evasion, as reflected by the increase in engraftment rate and regulation of macrophage infiltration in the tumor. Moreover, P1CP treatment resulted in a significant increase in metastasis formation in the head and tail of the zebrafish larvae, in MDA-MB-231 breast cancer tumors.

Overall, this project enhanced the knowledge on the biological effects of the presence of P1CP in the tumor microenvironment, confirming a role of this fragment in cancer cell invasion and metastasis formation and establishing an interaction with cells from the innate immune system which ultimately might contribute to immune evasion. Understanding the mechanism of action behind these pro-tumoral functions of P1CP could pave the way for the development of new targeted therapies to benefit cancer patients.

Resumo

O colagénio é o componente mais abundante da matriz extracelular, tendo um papel central na regulação do comportamento celular e do desenvolvimento do tecido e na providência de resistência à tração. No microambiente tumoral, o colagénio é mais rígido do que no estroma normal devido a um aumento da linearização e reticulação e um aumento na expressão de colagénio está correlacionado com um pior prognóstico.

Desmoplasia, um processo característico de vários tipos diferentes de cancro, incluindo cancro da mama, leva a um aumento da deposição de colagénio tipo I. A produção desta proteína resulta na libertação de P1CP, um marcador sensível para a atividade osteoblástica em metástases ósseas, com um valor de prognóstico relevante nesta doença. Contudo, as propriedades bioativas deste fragmento, em relação à progressão tumoral, permanecem pouco exploradas e podem representar uma área de estudo para desenvolvimento terapêutico. Este projeto teve como objetivo a exploração do papel biológico do P1CP na invasão e formação de metástases do cancro da mama bem como a interação deste fragmento com o sistema imune inato através de modelos *in vitro* de esferóides em 3D e de modelos *in viv*o de xenoenxertos de peixe-zebra.

Nos esferoides, formados com células de cancro da mama em co-cultura com células monocíticas ou macrófagos derivados de monócitos, o tratamento com P1CP levou a um aumento geral na capacidade invasora das células de cancro. Aumentos significativos na invasão de células de cancro na presença de monócitos THP-I e de macrófagos do tipo M0 e M1, apontam para um possível papel do P1CP na modelação da diferenciação de monócitos e na polarização de macrófagos para fenótipos pró-tumorais. As experiências realizadas nos xenoenxertos de peixe-zebra, realçam o P1CP como um possível agente na evasão imunológica, estando isto refletido pelo aumento na taxa de implantação e pela regulação da infiltração de macrófagos no tumor. Para além disto, tratamento com P1CP resultou num aumento significativo na formação de metástases na cabeça e cauda do peixe-zebra em tumores da linha MDA-MB-231.

No geral este projeto levou a um aumento do conhecimento dos efeitos biológicos da presença de P1CP no microambiente tumoral, confirmando um papel deste fragmento na invasão de células de cancro e na formação de metástases, bem como estabelecendo uma interação com células do sistema imune inato que pode contribuir para a evasão imunológica. A compreensão do mecanismo por detrás destas funções pró-tumorais do P1CP pode levar ao desenvolvimento de novos tratamentos direcionados contra o cancro.

Table of contents

List of figures

List of abbreviations

AVG: average

BC: Breast cancer

BM: basement membrane

BMP: bone morphogenic protein

BRCA: breast cancer susceptibility genes

CAAs: cancer-associated adipocytes

CSF1: colony-stimulating factor-1

CTCs: circulating tumor cells

DAMPs: damage associated molecular patterns

DDR: Discoidin Domain Receptors

DGAV: Direção Geral de Alimentação e Veterinária/Directorate General for Food and Veterinary

DMEM: Dulbecco's modified eagle medium

DPBS: Dulbecco's phosphate-buffered saline

ECM: extracellular matrix

CAFs: cancer-associated fibroblasts

EGF: epidermal growth factor

EMT: epithelial-mesenchymal transition

FBS: fetal bovine serum

FELASA: Federation of European Laboratory Animal Science Associations

FGF: fibroblast growth factor

hpf: hours post-fertilization

hpi: hours post-injection

IFN-γ: interferon-γ

LAIR-1: Leucocyte-associated immunoglobin-like receptor 1

LOX: lysyl oxidases

LPS: lipopolysaccharide

MCP-1: monocyte chemotactic protein-1 (CCL2)

MHC: major histocompatibility complex

MMPs: matrix metalloproteinases

MT1-MMP: membrane-type 1-matrix metalloproteinase

mTLD: mammalian tolloid

mTLL: mammalian tolloid-like

Nrp: neuropilin

ORBEA: Órgão de Bem-Estar e Ética Animal/Animal Welfare and Ethics Body

P1CP: procollagen type I carboxyterminal propeptide

P1NP: procollagen type I aminoterminal propeptide

PAMPs: pathogen associated molecular patterns

PDAC: pancreatic ductal adenocarcinoma

PDGF: platelet-derived growth factor

PDX: mouse patient-derived xenografts

PI3K: phosphoinositide 3-kinase

PMA: phorbol-12-myristate-13-acetate

PRRs: pattern recognition receptors

PVS: perivitelline space

RIA: radioimmunoassay

RPMI1640: Roswell Park Memorial Institute 1640

SEM: standard error of the mean

TAMs: tumor-associated macrophages

TCR: T cell receptors

TGF: tumor growth factor

TME: tumor microenvironment

TNF: tumor necrosis factor

VEGF: vascular endothelial growth factor

zPDX: zebrafish patient-derived xenografts

1 Introduction

1.1 Breast cancer epidemiology and risk factors

On a global scale, breast cancer (BC) remains the most commonly occurring type of cancer (2.261.419 cases, about 12.5% of total cases), as well as the main cause of cancer-related mortality among women (684.996, about 15.6%)[1]. However, incidence and mortality rates in women are significantly variable between different regions, with Europe presenting the second highest documented incidence (2.058.826 cases, about 22.3%)[1] and mortality (871.206 cases, about 19.7%)[1]. In Portugal, BC accounts for 27.8% of newly identified cancer cases and 15.7% of cancer-related deaths in women (figure 1.1)[1].

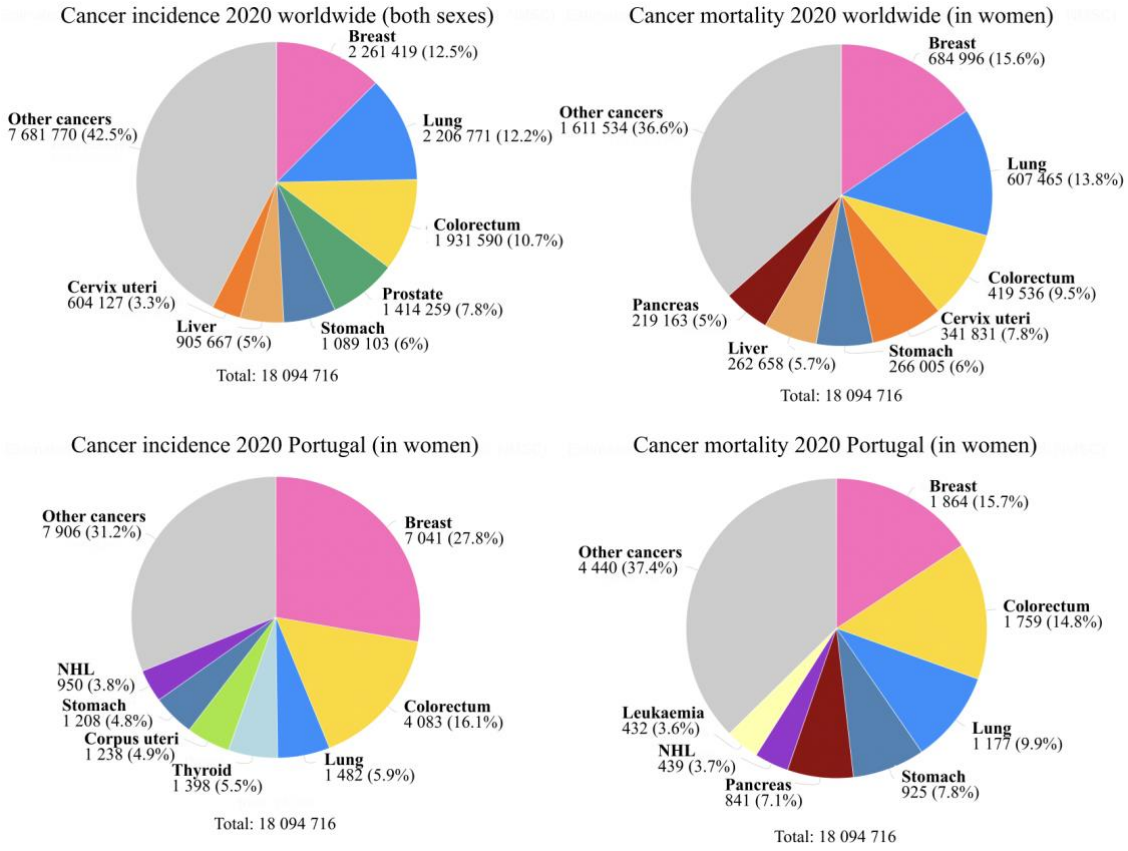

Figure 1.1. Breast cancer epidemiology. Cancer incidence in 2020, worldwide in both sexes (up left) - breast carcer represents 12.5% of the total number of cases. Cancer mortality in 2020, worldwide in women (up right) – breast carcer accounts for 15.6% of all cases. Cancer Incidence in 2020, in Portugal in women (down left) – breast cancer represents 27.8% of the total number of cases. Cancer mortality in 2020, in Portugal in women (down right) – breast cancer accounts for 15.7% of all cases. Retrieved from *Globocan*[1]

Breast epithelium is formed by a simple bilayer of inner luminal cells, responsible for milk production, and an outer layer of myoepithelial cells required for milk ejection. BC

mainly results from the unregulated growth of these epithelial cells[2] which can be stimulated by various established risk factors actively modulating the neoplastic transformation process of breast cells. These can be divided in a simplistic manner into 3 categories: nongenetic and nonmodifiable, nongenetic and modifiable and genetic risk factors[3]. The first group includes inherent factors namely age, race, early menarche/late menopause, BC history (reoccurrence) or benign proliferative lesions of the mammary gland[3]. The second group includes extrinsic factors determined by lifestyle such as education, changing of reproductive patterns, menopausal hormone use, tobacco, alcohol or fitness and nutrition[3]. Genetic risk factors are normally associated with genetic mutations in one of two Breast CAncer (BRCA) susceptibility genes, BRCA1 and BRCA2, which cause approximately 3% of all BCs[4]. Nevertheless, and in spite of intensive studies leading to the identification of these risk factors, in 75-80% of all BC cases in women no risk factor is found[5].

1.2 Breast cancer subtypes

Breast tumors' behavior and the ability to respond to different types of therapy is highly dependent on tumor molecular characteristics and distinct patterns of gene expression. Therefore, identification of the several subtypes of breast tumors might be of very important clinical relevance in leading to a more accurate prediction of therapy response and prognosis. Methods such as histopathology, molecular pathology and genetic analysis allowed for the recognition of five main molecular subtypes of BC: luminal A, luminal B, triple-negative/basal-like, HER2-enriched and normal-like[6,7].

Luminal A is the most common molecular subtype of BC[8]. It is characterized by being hormone-receptor positive (estrogen receptor and/or progesterone receptor positive), HER2 negative, and has low mitotic activity[8]. Luminal B is also hormone-receptor positive and can be HER2 positive or negative but has a higher proliferative index, leading to a slightly faster tumor growth[8]. Triple-negative BCs are highly aggressive and present the worse short-term prognosis[9]. They are hormone-receptor negative, as well as HER2 negative[9]. HER2-enriched BC is HER2-positive and is highly proliferative, presenting a more aggressive biological and clinical behavior[8]. The normal-like molecular subtype is similar to luminal A, being hormone-receptor positive and HER2 negative, and it is characterized by a normal breast tissue profiling[10].

1.3 Tumor microenvironment

The tumor microenvironment (TME) is defined by a complex network of interactions between cancer resident, stromal and infiltrating host cells and the surrounding extracellular matrix (ECM). This intercellular communication and cancer cell's ability to acquire new genetic and molecular characteristics allow the tumor to develop, progress and evade the host's defense mechanisms[11]. In an attempt to organize these cancer properties, in 2011, Hanahan and Weinberg defined 8 hallmarks of cancer, including tissue invasion and metastasis and the ability to evade immune response[12]. Research focusing on the characterization of these hallmarks may help for a better understanding of TME dynamics and tumor development in general.

Cellular components present in the TME include immune cells (T cells, B cells, macrophages, dendritic cells, NK cells, neutrophils) commonly associated with a good prognosis but recently identified as interacting with transformed cells to promote oncogenesis[13,14] by generating an immunosuppressive environment. Other cells are present in the TME, such as endothelial cells which form new vessel structures for nutrient delivery, gas exchange and withdrawal of metabolites for growth, cancer-associated fibroblasts (CAFs) that promote tumorigenesis, migration, and survival[15,16], and cancer-associated adipocytes (CAAs) which induce a chronic inflammatory environment by inflammatory cytokine production[17]. Moreover, cancer cells interaction with the tumor stromal ECM also promotes cancer progression, by influencing cell behavior (figure 1.2)[18]. The interaction of cancer cells with these components dictates tumor-suppressive or tumor-promotive events, strongly influencing tumor development and cancer cell proliferation and invasion.

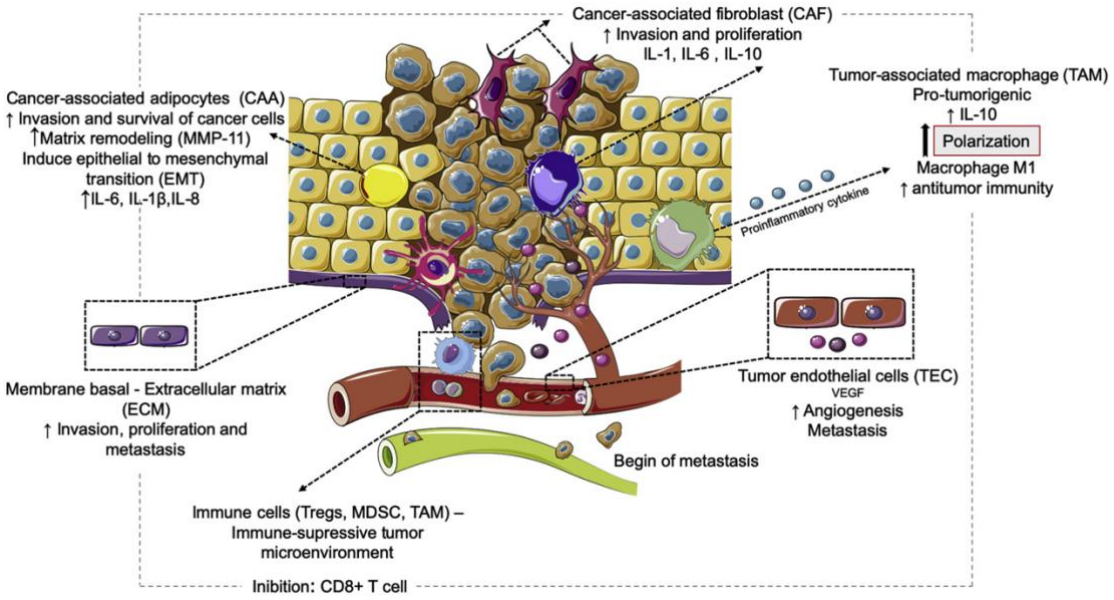

Figure 1.2. Tumor microenvironment components and respective functions in tumor development. Immune cell infiltration in the TME generates an immunosuppressive environment promotor of cancer cell survival. Recruitment of endothelial cells induces angiogenesis, defined by the formation of new vessels, by the influence of pro-angiogenic molecules and the vascular endothelial growth factor (VEGF). CAFs promote tumor growth, invasion, and angiogenesis. Cancer-associated adipocytes produce IL-6 leading to a chronic inflammatory environment, facilitating invasion and tumor progression. The ECM has essential functions in cancer cell invasion and metastasis formation. Adapted from *Ribeiro Franco et al. (2019)*[17].

1.4 The extracellular matrix

1.4.1 Primary components and features of the extracellular matrix

The ECM is formed by a large collection of biochemically distinct components including collagens, proteoglycans, elastin, and glycoproteins such as laminin and fibronectin[19]. These components comprise the basement membrane (BM), produced by epithelial, endothelial, and stromal cells to separate epithelium or endothelium from stroma, and the interstitial matrix, mainly produced by stromal cells[18]. The BM has a particular composition containing type IV collagen, laminins, fibronectin, and linker proteins, responsible for the connection between collagen and other proteins. It has an important role in epithelial cell function, establishing the orientation that maintains apicobasal polarity and cell differentiation[20]. The interstitial matrix is richer in fibrillar collagens, mainly type I collagen, proteoglycans, and several glycoproteins, providing the tensile strength of the tissue[21].

Collagens are the main structural elements of the ECM and have pivotal roles in regulating cell adhesion, supporting chemotaxis and migration, directing tissue

development, and providing tensile strength[22]. Collagen is composed of 3 polypeptide α chains that upon formation are organized in a triple-stranded helix which can be assembled into fibrils or networks, depending on the type of collagen[23]. Fibrous collagens constitute the mainstay of collagen fibril bundles within the interstitial matrix and network collagens are present in the BM[24]. Fibril-forming collagens, such as type I collagen, suffer several post-translational modifications, namely the hydroxylation of proline and lysine residues, glycosylation of lysine and the cleavage of N- and C-terminal propeptides (non-collagenous domains)[24]. Following this processing, resulting collagen fibrils are strengthened by the covalent crosslinking of lysine residues by lysyl oxidases (LOX)[25].

1.4.2 Extracellular matrix in tumor development

It is now understood that the ECM has major roles in the maintenance of tissue homeostasis and in regulating cell proliferation, apoptosis, adhesion, and migration. Therefore, a failure in the regulation of ECM dynamics, specifically remodeling, could massively affect its properties and functions, influencing cell behavior. This regulation is assured by the control of ECM deposition by stromal cells, namely fibroblasts, and the expression and function of ECM degrading enzymes, such as matrix metalloproteinases (MMPs) and their inhibitors[26]. In cancer, this balance is disrupted culminating in an abnormal quantity, composition, and topography of the ECM, highlighting a continuous interaction between the tumor cells and the surrounding matrix[26]. This interaction often leads to increased secretion and accumulation of deposited ECM proteins referred to as fibrosis[26].

Initially, cancer cells recruit and activate stromal cells, the main depositors of ECM components in the TME. This recruitment is achieved by the release of several pro-fibrotic growth and inflammatory factors including tumor growth factor (TGF)-α, TGF-β, fibroblast growth factor (FGF)-2, platelet-derived growth factor (PDGF) and epidermal growth factor (EGF)[27]. These factors also induce the differentiation of stromal cells into CAFs which function as myofibroblasts, the activated form of fibroblasts, remodeling the ECM to support tumor progression[28]. In BC, CAFs are induced by pre-tumoral cells to undergo epigenetic changes and alter the molecular composition of the ECM, mainly through an increase in the deposition of collagen, fibronectin, and tenascin, and by increasing the presence of inflammatory cytokines and growth factors, namely VEGF and

CXCL-12, which alter cell behavior by promoting cell proliferation and an invasive phenotype as well as stimulating vascular growth[29].

ECM degradation is also altered in tumorigenic conditions. Tumor and stromal cells express excessive levels of ECM-degrading enzymes, such as MMPs, that act on several steps of tumor growth[30]. Degradation of ECM components by these enzymes allows destruction of normal ECM which is replaced by tumorigenic ECM and is a main driver of cancer cell motility[28]. Furthermore, an increase in protease activity leads to the release of several signaling molecules like growth factors, normally attached to the ECM, improving their bioavailability to tumor cells[28]. In BC, MMP-9 overexpression is a characteristic of triple-negative and HER2-positive BCs and is also found in metastatic lymph nodes, being associated with malignancy and a poor prognosis[31]. Furthermore, both MMP-9 and MMP-2 expression levels correlate with lymph node metastasis and tumor staging in BC tissues, being used as references for prognosis and treatment[32].

1.4.2.1 Role of collagen in tumor evolution

Collagens constitute the most significant component of the ECM and consequently have a central role in the functional properties of the matrix. An imbalance in the deposition and degradation rates of collagen can lead to the loss of ECM homeostasis[19].

In cancer, ECM's biomechanical properties are altered and frequently tumor stroma is stiffer than normal stroma[18]. This stiffness is due to a physical restructuring of the interstitial collagen, marked by its' increased linearization and crosslinking[33]. Additionally, one of the features of many carcinomas, particularly breast[34] and pancreatic ductal adenocarcinoma (PDAC)[35], is the process of desmoplasia, characterized by the presence of a dense collagenous stroma, rich in interstitial fibrillar collagen (type I and III) and the increased degradation of type IV collagen.

Linearization of interstitial collagen arises normally through an increase in collagen crosslinks. As mentioned above, collagen crosslinking mainly occurs in an enzyme-mediated fashion, through the action of LOX enzymes which are upregulated in cancer[36]. During early stages of carcinogenesis, LOX enzymes are produced by stromal cells but in later, more advanced stages they are synthesized by tumor cells in response to hypoxia[37]. The resulting increase in ECM stiffness mediates the activation of integrins and elevates Rho-generated cytoskeletal tension promoting focal adhesion formation and cell motility[18]. Furthermore, excessive activity of LOX enzymes has been clinically

linked with tumor progression and metastasis promotion[38]. Interestingly, LOX activity found on invasive edges of tumors has been shown to drive actin polymerization, cell contractility, and migration, providing a pathway for tumor cells to follow[19]. Indeed, linearized, and stiffer collagen fibers were shown to serve as migratory tracks for tumor cells to travel through the interstitial matrix[39]. Accordingly, the signature of highly aligned collagen fibers is associated with poor prognosis, particularly in BC[40].

Collagens can also directly trigger cellular signaling cascades by binding transmembrane receptor tyrosine kinases called Discoidin Domain Receptors (DDR1 and DDR2)[41]. In BC, the binding of type I collagen to DDR1 in tumor cells induces stemness-like signaling by activating transcription factor STAT3, which mediates metastatic outgrowth[42]. Moreover, in gastric cancer, DDR1 expression is associated with cancer cell invasion and metastasis formation[43].

1.4.2.2 Role of extracellular matrix remodeling in tumor cell invasion and metastasis formation

In the early stages of tumor development, neoplastic cells are separated from the surrounding stromal cells by the BM that prevents cancer cell dissemination. The tumor turns malignant when tumor cells acquire the ability to grow uncontrollably and move into the interstitial space, breaking the BM, and invading the surrounding tissues[28]. This process is made possible by modulation of ECM remodeling mainly by the degrading action of proteases. For example, in BC the BM is degraded by membrane-anchored proteases, namely membrane-type 1-matrix metalloproteinase (MT1-MMP), allowing tumor cell breakthrough[44]. CAFs also play a big role in the latter by applying physical force in the BM and widening the holes created by proteases thus promoting cell invasion (figure 1.3)[45].

Degradation of the ECM by proteases is an essential step in the movement of cells through the interstitial matrix as it opens a migratory channel and reduces mechanical stress on the migrating cells[46]. In tumors, which normally have a dense collagenous stroma, as explained above, proteolysis of the ECM is a key step in cancer cell migration and is performed by MMPs, mainly MT1-MMP, and MMP-producing cells such as CAFs, which degrade the collagen migration barriers[28].

Metastasis formation depends on the local niche promotion of tumor development at the primary site and on a metastasis niche that confers optimal conditions for invading

cancer cells to survive, colonize and expand[18]. Beyond the role in tumor cell dissemination, the ECM also constitutes an essential component of the pre-metastatic and the metastatic niches.

The primary tumor induces an ideal microenvironment at the distant tissue, through processes such as ECM remodeling, assuring ideal pro-tumoral conditions even before the presence of metastatic tumor cells, leading to the formation of the pre-metastatic niche[28]. This is achieved through the release of primary tumor-derived factors that activate stromal cells at the pre-metastatic site which in turn modify the composition and organization of the ECM[28]. For example, in bone metastasis formation of BC, primary tumor-derived factors usually generate an osteolytic (bone-degrading) pre-metastatic niche through modulation of bone homeostasis by promoting the activity of bone-resorbing osteoclasts by factors such as tumor-derived LOX[28,47]. Moreover, the primary tumor also induces recruitment and adhesion of immune populations to the pre-metastatic niche, namely macrophages, neutrophils, and myeloid progenitor cells that, by remodeling the ECM, promote colonization of metastatic tumor cells[48]. Importantly, MMPs secreted by cancer cells, such as MMP-3 and MMP-10, are capable of promoting the extravasation of circulating tumor cells (CTCs) and an increase in ECM degradation, facilitating the infiltration of tumor cells and bone marrow-derived cells in the pre-metastatic niche[49].

Upon colonization of the pre-metastatic niche, stromal and tumor cells actively modulate ECM remodeling to guarantee the best possible conditions for metastasis formation, establishing the metastatic niche[28]. This process involves the deposition of specific proteins by stromal or tumor cells, such as several types of glycoproteins (osteopontin, periostin and tenascin C) which aid the colonization of tumor cells through the activation of stemness-like signaling pathways[50,51].

The epithelial- mesenchymal transition (EMT) in an essential process for cancer cells to acquire the ability to invade and metastasize, involving the loss of epithelial features, namely cell-cell adhesion molecules (E-cadherin, cytokeratin, tight junction protein 1) and apicobasal polarity, and the gain of mesenchymal characteristics such as increased mobility, elevated resistance to apoptosis and expression of specific cell markers (vimentin, N-cadherin, fibronectin, MMPs)[52]. Accordingly, CTCs display a mesenchymal phenotype whereas primary tumor and established metastatic cells reveal an epithelial phenotype[53]. Bone marrow-derived cells were demonstrated to promote this transition of

metastatic cells from a mesenchymal to an epithelial phenotype through the deposition of versican[54], highlighting the metastatic promoting abilities of this proteoglycan.

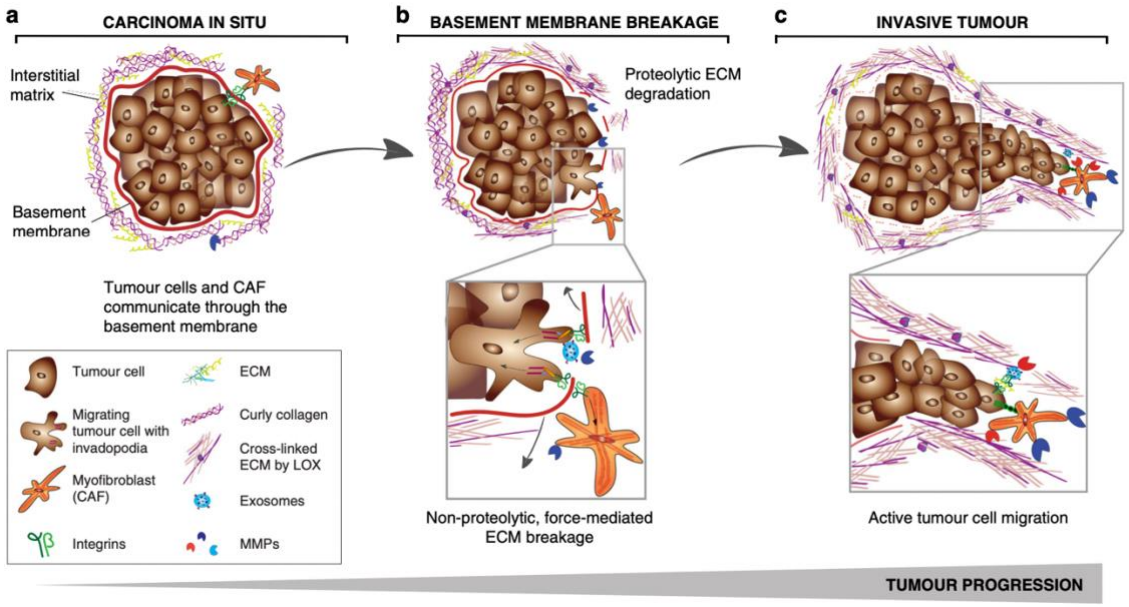

Figure 1.3. ECM remodeling in tumor cell invasion. a In the primary tumor, cancer cells are restricted by the BM which prevents invasion of the surrounding tissue. **b** BM breakage occurs through ECM degradation by the proteolytic activity of tumor and stromal cell-secreted proteases or by non-proteolytic force-mediated ECM remodeling. **c** LOX enzymes, secreted by tumor cells and CAFs, increase collagen crosslinking and linearization. Invading tumor cells migrate alongside the linearized collagen fibers, serving as migratory tracks. Tumor cell and CAFs-secreted MMPs, such as the MT1-MMP, degrade collagen migration barriers. Adapted from Winkler *et al.* (2020)[28].

1.4.2.3 Matrikines

A relevant process of ECM degradation is the cleavage of long ECM components which gives rise to bioactive, shorter fragments with structure and functions similar to chemokines and cytokines, termed matrikines[55,56]. These fragments present distinct functions to the ones attained by the full-length ECM component which could be pro- or anti-tumorigenic[28]. Matrikines cleaved from fibronectin, collagen, laminin, elastin, and other matrix related molecules have been demonstrated to have an active role in tumor progression, having an effect in cell proliferation, migration, protease production or apoptosis[28].

In this regard, several matrikines have been already characterized, including collagen-derived matrikines. DGGRYY, present in the C-terminal telopeptide of the α1 chain of type I collagen is an activator of polymorphonuclear neutrophils[57]. The tripeptide GHK, present in the α2(I) chain of type I collagen displays high affinity for copper (II) ions, and together they form a tripeptide–copper complex (GHK–Cu)[58] which has several abilities

including acting as a chemoattractant of monocytes/macrophages[59], stimulating angiogenesis *in vivo*,[60] increasing ECM synthesis[61] and modulating ECM remodeling by the increase of expression and activation of A/MMP-2[62]. Relevant matrikines are correspondent to several NC1 domains of BM collagens such as the 185-203 and 54-132 peptides of the C-terminal domain of the α3 chain of type IV collagen. The former has shown ability to inhibit human polymorphonuclear neutrophils[63], decrease tumor cell proliferation[64], and inhibit tumor cell migration through the downregulation of MT1-MMP or MMP14 and integrin β3[65]. The latter demonstrated anti-angiogenic properties[66] also displayed by other collagen-associated matrikines like endostatin, a C-terminal domain of type XVIII collagen[67].

1.5 Type I procollagen carboxyterminal propeptide (P1CP): What have we learned so far?

Type I collagen, the most abundant collagen in the human body, is an essential part of the connective tissue[68]. It is the major component of the matrix in the bone comprising 90% of its composition where it is synthesized by osteoblasts[69]. Procollagen type I, its biosynthetic precursor, has additional aminoacidic sequences at both ends, the NH_2-terminal (PINP) and the COOH-terminal (P1CP) propeptides. Upon type I collagen assembly, procollagen type I undergoes a series of post-translational modifications including cleavage of the propeptides performed by specific proteases (figure 1.4)[70]. Processing of P1CP is achieved by four bone morphogenic protein (BMP1)-like proteinases: BMP-1, mammalian tolloid (mTLD), and mammalian tolloid-like 1 and 2 (mTLL1 and 2). Interestingly, BMP-1 was shown to have the highest P1CP cleavage efficiency *in vitro*[71].

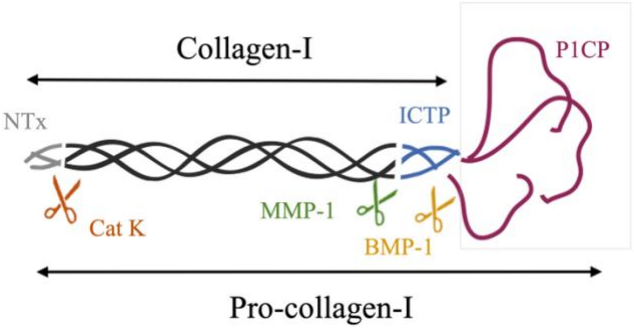

Figure 1.4. Simplified scheme of the relative localization of the different fragments on the type I collagen molecule and enzymes responsible for their generation.

After processing, the propeptides are released and the mature collagen molecules are assembled into fibrils[72,73]. However, while P1CP is completely cleaved and released in equimolar amounts to the newly synthesized collagen in any tissue, P1NP can be retained in fibers in soft tissues or released in a degraded form[72]. Accordingly, the concentration of P1CP in the blood is a main direct indicator of type I collagen synthesis and assembly[73].

P1CP is a globular polypeptide with intrachain and interchain disulfide bridges and a high molecular weight of 100 kDa[73]. Due to its size, this molecule is not filtered by the renal glomeruli and is instead eliminated by hepatic endothelial cells via the mannose endocytic receptor[74]. In 1974, Taubman *et al*. introduced the first assay for P1CP serum measurement in the form of a radioimmunoassay (RIA) which led to several studies that revealed variances in P1CP serum levels in metabolic bone diseases[75]. This method was later modified and allowed further studies that confirmed a strong positive correlation between serum P1CP levels and new bone formation[76]. Interestingly, high concentrations of this molecule were also encountered in patients of various bone-related diseases such as Paget's bone disease and osteoporosis[77].

Following these findings, together with the aforementioned studies regarding P1CP and bone formation, research carried out by Francini *et al.* in 1993 reported serum levels of P1CP as a sensitive marker for osteoblastic activity in patients with bone metastasis[70]. Furthermore, and since bone metastasis represents the most prevalent form of metastasis in breast carcinoma, Jukkola *et al*. decided to evaluate serum concentrations of P1CP and P1NP in BC patients. RIA demonstrated that increased concentrations of both propeptides were verified in patients with aggressive disease suggesting that procollagen type I metabolism is associated with poor clinical outcomes[73]. Interestingly, serum levels of P1CP were also shown to be useful indicators for bone metastasis prediction in prostate cancer[78].

Several previously unknown functions of P1CP were illustrated by Palmieri *et al*. which indicated a possible epigenetic role of this molecule in promoting breast tumor progression and vascularization[79]. Indeed, P1CP was firstly shown to be chemoattractant for endothelial cells *in vitro*, hinting a possible role in endothelial cell migration and vascularization of collagen type I- producing tissues[79]. Furthermore, studies performed in MDA-MB-231 cells reported that P1CP was able to induce the directional migration and proliferation of these cells as well as promote the expression of TIMP-2, and pro-MMP-2 and -9[80]. Following these discoveries, in an attempt to clarify the role of P1CP in tumor

progression, Palmieri *et al*. demonstrated that the molecule was capable of activating pro-angiogenic and pro-migratory signaling cascades in MDA-MB-231 cells. This was demonstrated by the ability to induce the expression of VEGF-A, a major angiogenic factor, and activate a positive autoregulatory VEGF loop involving the Neuropilin (Nrp)-1 receptor, required for breast carcinoma invasion *in vitro*. Moreover, P1CP was shown to increase the expression of CXCR4, a receptor part of the CXCR4/CXCL12 paracrine loop which is involved in tumor cell invasion[80].

The results obtained *in vitro*, led to the hypothesis that P1CP could promote tumor vascularization and progression *in vivo*. Accordingly, Visigalli *et al*. generated BC cell xenografts using BalbC/nude mice in which they implanted MDA-MB-231 cells added or not with P1CP, purified from serum free medium conditioned by mature rat osteoblasts[29]. The presence of the latter resulted in more vascularized tumors, up-regulation of pro-metastatic genes (VEGF-A, MMP-9 and CXCR4), and down-regulation of the tumor inhibitory gene *RECK*, responsible for the inhibition of MMP-9, MMP-2 and MT1-MMP. These results pointed to a role of P1CP in the promotion of tumor progression *in vivo*, by the induction of expression of genes associated with metastasis formation and vascularization[29].

1.6 The immune system

As mentioned above, the TME is composed, besides cancer cells, by other cell types including cells of the immune system. Immune cell infiltration has been proven to play an essential role in tumoral development and progression, as well as metastasis formation[81]. The immune system can be divided into two different types of immunity: innate immunity and adaptive immunity, which offers constant protection to the individual. Innate immunity is the first to act in presence of a threat and is non-specific, acting through soluble factors such as complement molecules, chemokines, and cytokines, as well as myeloid cells, like macrophages and neutrophils, and even some lymphoid cells – NK and γδT lymphocytes[82].

Innate cells express Pattern Recognition Receptors (PRR's) that recognize the Pathogen Associated Molecular Patterns (PAMP's) and the Damage Associated Molecular Patterns (DAMP's) that come from an infection or a disease. After being activated, the PRR's guide inflammatory cytokines release and complement cascade activation[82].

The bridge between innate immunity and adaptative immunity is executed by the presentation of antigens to adaptive T cells by dendritic cells and macrophages. The presentation occurs through the Major Histocompatibility Complex (MHC) at the surface of each cell, which are then recognized by the T cell receptors (TCR) in adaptive T cells membranes[82].

1.6.1 Tumor-associated macrophages (TAMs)

Macrophages are cells of the innate immune system that descend from the myeloid lineage. They are a heterogeneous immune population, and their phenotype and functions are tightly regulated by the environment of the surrounding tissue[83]. The majority of tissue-resident macrophages originate from embryonic precursor cells, but they are sometimes replaced or complemented by monocyte-derived macrophages. In adult pathophysiological conditions, macrophages are mostly derived from monocytes[83].

Within the TME, macrophages are present in every stage of tumorigenesis, accounting up to 50% of tumoral mass and present distinct roles throughout carcinogenesis and metastasis development[84].

Initially, macrophages are anti-tumoral and pro-inflammatory, but in later, more advanced stages, they become pro-tumoral. This plasticity and acquisition of different phenotypes presented by macrophages are influenced by stimuli from the TME[85]. Therefore, macrophages can be divided, in a simplistic way, between 2 types or polarization states: M1 and M2, which correspond to the extreme opposite phenotypes of a spectrum of responses[81].

M1 macrophages, or classically activated macrophages, are pro-inflammatory and have an aggressive phagocytic function. They produce effector molecules (e.g., tumor necrosis factor (TNF)-α and ROS) and important inflammatory cytokines such as IL-12 and IL-23. Low production of IL-10, an anti-inflammatory cytokine, is also a characteristic of the presence of this type of macrophage. High production of IL-12 leads to the activation and clonal expansion of Th17 cells, that secrete IL-17, promoting an inflammatory process. Through production of chemokines, CXCL9/Mig and CXCL10/IP-10, M1-type macrophages attract Th1 lymphocytes, leading to an immune response normally associated with microbial infections[84,85]. M1 macrophages can be polarized by inflammatory signals such as IFN-γ, TNF-α, IL-1β and LPS *in vitro*[81].

M2 macrophages, or alternatively activated macrophages, are anti-inflammatory and have essential roles in angiogenesis and tissue repair[81]. In contrast to M1 macrophages, they are not capable of antigen presentation[81]. They express high levels of IL-10 which acts in the activation of Th2 response, leading to increased IL-3 and IL-4 expression. Secretion of IL-4 is involved in ECM production, essential for healing processes[86]. Polarization into M2 macrophages is more complex, as there are several subsets that can be induced by different signals and molecules: M2a macrophages are responsible for Th2 response and type II inflammation and their polarization is triggered by IL-4 and IL-13; M2b macrophages also participate in Th2 activation and immune regulation and are polarized through the activation of TLRs and immune complexes; M2c macrophages are involved in immune suppression, tissue repair, and ECM remodeling and are stimulated by IL-10 or TGF-β; M2d macrophages are correlated with tumor progression by angiogenesis promotion, through TGF-β and VEGF secretion, and are induced by IL-6[81,87].

The majority of TAM's present in the TME acquire the M2 phenotype which in general enhance tumoral proliferation and angiogenesis and suppress antitumoral immunity[84]. TAMs are derived from circulating monocytes or tissue resident macrophages that are recruited to tumor sites by several microenvironmental signals in the form of cytokines, chemokines, ECM components, and hypoxia. The main regulators of monocyte/macrophage recruitment to the tumor are cytokines, chemokines or growth factors released by tumor or stromal cells from the TME such as colony-stimulating factor-1 (CSF1) and CCL2 (monocyte chemotactic protein-1; MCP-1)[88]. Indeed, elevated CCL2 levels correlate with macrophage accumulation in various human cancers, namely BC, and in human metastatic BC high CSF1 levels are associated with increased macrophage infiltration[88,89].

TAMs are highly involved in the metastatic process through the production and secretion of growth factors, proteolytic enzymes, and several immune inhibitory checkpoint proteins[90]. They act in almost all steps of metastasis formation from the escape of tumor cells from the primary site to the establishment of the pre-metastatic niche. In the initial step of invasion, TAMs have been proven to be involved in the EMT process by secreting soluble factors such as TGF-β. Moreover, they are capable of ECM degradation through the production of proteolytic enzymes such as cathepsins, MMPs, and serine proteases[90]. Importantly, TAMs, mainly with the M2 phenotype, have the ability to secrete pro-angiogenic factors, such as FGF, VEGF-A and adrenomedullin[88],

leading to increased tumor vasculature. Intravasation to these surrounding blood vessels relies on a paracrine loop where tumor cells produce CSF-1 to induce macrophage motility and TAM-derived EGF production which mediates chemotactic migration of tumor cells to the blood vessels[90]. Finally, recent studies have demonstrated a significant contribution of macrophage recruitment in the formation of the pre-metastatic niche and in the survival of tumor cells at the metastatic site, mainly through ECM remodeling via secretion of MMPs, integrins and LOX enzymes and immunosuppression by establishing a metabolic crosstalk with Th1 and dendritic cells[90].

In BC, enhanced TAM recruitment is correlated with poor prognosis, high tumor grade, low estrogen and progesterone receptor status and high tumor mitotic activity[91]. Latest research in this matter found a role for TAMs in BC cell proliferation through activation of phosphoinositide 3-kinase (PI3K)-Akt signaling, as well as apoptosis inhibition through increased Bcl-2 and decreased Bax expression[92]. Moreover, Maller *et al.* described a subset of CD163/RELMα-positive TAMs that, through secretion of TGF-β, are actively involved in LOX/LH2-dependent collagen crosslinking, stromal stiffening, and fibrosis strongly correlated with aggressive breast tumors[93]. Importantly, highlighting the importance of TAMs in BC metastasis, a subset of monocyte-derived bone metastasis-associated macrophages were proven critical for bone metastasis outgrowth in BC patients in an IL4R-dependent manner[94].

1.7 3D spheroids as models to study tumor behavior

The ideal *in vitro* model, considering all the interactions established between several tumoral components and the surrounding ECM, must be selected in order to best recapitulate the TME *in vitro*. In preclinical studies, a relevant method employed to achieve this is spheroid formation from cell cultures[95]. Spheroids are sphere-like cell aggregates with a 3D organization that can be assembled with different cell types (heterospheroids) or with the same cell type (homospheroids). Accordingly, spheroids formed by cancer cells can be solely comprised by these cells or co-cultured with other cell types, namely fibroblasts, endothelial cells, or immune cells[95], allowing a certain degree of TME cellular representation. In contrast with 2D *in vitro* cell cultures, in which cells are grown in a monolayer, tumor spheroids are able to more closely mimic *in vivo* cell-cell interactions, ECM production and deposition, ECM-cell interactions and cell behavior[96]. Indeed, cells within this structure reportedly deposit ECM components such

as collagen, laminin, fibronectin and proteoglycans and present ECM-cell (5- and 1-integrin) and cell-cell physical contacts (e.g., E-cadherin). These interactions trigger signaling pathways also active in solid tumors that confer tumor cells resistance to anti-cancer drugs[95] and are heavily involved in ECM remodeling, essential in cancer cell migration[18]. Moreover, 3D tumor spheroids are able to replicate, to an extent, the growth pattern, multilayer cellular organization, and gene expression profile found in solid tumors *in vivo*[95].

Several techniques have been developed to allow the characterization of different properties of 3D tumor spheroids including size, protein and gene expression, cell proliferation and death, the invasive potential of cancer cells and their resistance to anticancer drugs[95,97]. Currently, optical microscopy, specifically confocal laser scanning microscopy, constitutes the main option for the study of these features as it allows, together with staining protocols, the observation of the spatial organization, spheroid growth, and state of the cancer cells. The latter is achieved by the use of antibodies which target specific proteins (e.g., caspase-3, Ki-67) and biomarkers[95]. Furthermore, techniques such as flow cytometry, western blot and qRT-PCR can be used to characterize cell populations within the spheroid as well as patterns of specific gene and protein expression[95].

1.8 Zebrafish xenografts: novel tool for *in vivo* studies in cancer research

For accurate comprehension of tumor progression and development of new treatments, usage of preclinical models is increasingly essential. Cells obtained from cancer patients have been adapted to grow in artificial conditions and subcutaneous injection of these cells in immunodeficient mice constitutes the main *in vivo* model for preclinical drug testing[98]. Mouse patient-derived xenografts (PDX) are an advanced preclinical model that has allowed to establish a correct correlation between tumor development, upon drug treatment in the mouse, and the patients' response to the same drug[98]. However, PDX models are not perfect, presenting two major setbacks regarding tumor engraftment time frame (2 months) and the number of cells required from the patient.

Zebrafish xenografts are innovative *in vivo* models for human cancer research that have been proved valuable for studies regarding the molecular biology of the tumor and, more recently, serving as a screening tool for therapeutic options in several cancer types

in the form of zebrafish patient-derived xenografts (zPDX)[99–101]. In contrast to mouse PDX, they are a high-throughput and low-cost model having a hatching rate of about 150-200 eggs per week, they present a reduced engraftment time rate and a much larger number of possible transplants (~300/hour). Moreover, in larvae stage transparency allows real-time imaging with cellular resolution, and the availability of several transgenic lines and mutants enables the study of specific pathways, cells, proteins, and genes[102].

Recently, zebrafish xenografts have been used in the research of several aspects of tumor biology, specifically tumor-driven angiogenesis, metastasis formation and the interaction between the tumor and the immune system[103–105]. This is due to a high conservation of cancer-related molecular signaling pathways between zebrafish and humans regarding cell proliferation, migration, apoptosis, and differentiation[106]. Furthermore, various oncogenes and tumor suppressor genes involved in tumor formation have been found to have zebrafish homologs[106]. Zebrafish also possess a particularly conserved vertebrate innate immune system which comprises complement, Toll-like receptors, neutrophils, and macrophages[105]. Interestingly, this system is active right after fertilization whereas the adaptive immune system only reaches full functional maturation at 4-6 weeks post-fertilization. This allows for an interval in which the study of innate immunity could be done independently of the adaptive immune response[107].

2 Objectives

In this project we focused on the understanding of TME dynamics, exploring the role of P1CP in BC cell invasion and metastasis formation, as well as in the recruitment, and function of TAM-like cells. To do this, we selected BC cell lines – MDA-MB-231, MDA-MB-231 BO2[108] and MDA-MB-231 BrM[109] and a human monocytic cell line – THP-I that we successfully differentiated and polarized into the different subsets of macrophages. We developed two different cancer models: a 3D spheroid *in vitro* model and *in vivo* zebrafish larvae xenografts.

In vitro with the 3D spheroid model, we intended to:

- Assess if cancer cells' invasive ability is affected in the presence of P1CP upon co-culture with monocytes, M0-, M1-, or M2-like macrophages.

In vivo using zebrafish xenografts, we aimed to:

- Determine if treatment with the P1CP fragment has an effect in cancer cells' metastatic potential;
- Analyze if macrophage recruitment is observed under the same treatment.

3 Materials and Methods

3.1 Cell lines and culture

BC cell lines GFP-expressing MDA-MB-231, MDA-MB-231 BrM and MDA-MB-231 BO2, and a THP-I monocytic cell line, were employed. BC cell lines were cultured in high glucose (4,5 g/L) DMEM (Dulbecco's Modified Eagle Medium) (Gibco) supplemented with 10% fetal bovine serum (FBS) (Biowest) and 1% Penicillin-Streptomycin (HyClone). THP-I monocytic cell line was cultured in RPMI1640 (Gibco) supplemented with 10% FBS (Biowest) and 1% Penicillin-Streptomycin (HyClone). All cell lines were cultured in a humidified atmosphere containing 5% CO_2 at 37°C and were tested for mycoplasma. Monocytic cell line THP-I was obtained from Luís Moita Lab at Instituto Gulbenkian de Ciência (IGC). BC cell line MDA-MB-231 was provided by Sérgio Dias Lab at Instituto de Medicina Molecular (iMM), BC cell line MDA-MB-231 BO2 was provided by Phyllippe Clézardin Lab, *Institut National de la Santé et de la Recherche Médicale* (INSERM) and BC cell line MDA-MB-231 BrM was kindly supplied by Patrícia S. Steeg and David Lyden Lab at Cornell University.

3.2 Cryopreservation and cell storage

Cells with 2-4 passages were frozen to avoid accumulation of mutations *in vitro*. Freezing medium for BC cells was prepared by adding to DMEM, 10% FBS and 10% DMSO, in which the cells were resuspended. The freezing solution for THP-I cells consisted solely of DMSO containing 10% FBS. The final solution of cells + freezing medium was equally distributed between cryovials that were placed in a cryobox with isopropanol and then moved to a -80°C freezer overnight. The cryovials were then transferred into the liquid nitrogen tank where they remained stored for later use.

3.3 Cell thawing

The cryovials containing frozen cells of interest were removed from the liquid nitrogen and immediately placed in a 37°C water bath for quick thawing. The vial with already thawed cells was then transferred to the laminar flow hood. The adequate amount of complete growth medium was pre-warmed and added in the 15 mL falcon tube already with the cells. The cell suspension was then centrifuged (177 g, 5min) and the supernatant

removed. Cells were resuspended in complete growth medium, added to a cell culture flask, and placed in an incubator at 37°C and 5% CO_2.

3.4 THP-I differentiation and polarization

THP-I cells were counted and plated at $1x10^6$ cells/mL considering 4 different conditions: THP-I control; THP-I + phorbol-12-myristate-13-acetate (PMA) (Enzo Life Sciences); THP-I + LPS (Merck Life Sciences) and IFN-γ (PrepoTech); THP-I + TGF-β1 (ProDots®, R&D Systems). Monocytes from all conditions, except THP-I control, were exposed to PMA (20ng/mL) for 24h and were incubated at 37°C and 5% CO_2, for differentiation into macrophages. The medium was replaced with supplemented RPMI1640 medium 1h before the next treatment. Cells were then kept for 48h in this medium for M0-like macrophages (THP-I + PMA condition), with a polarizing treatment of LPS (100 ng/mL) and IFN-γ (50 ng/mL) for M1-like macrophages (THP-I + LPS and IFN-γ condition), and with TGF-β1 (20 ng/mL) for M2-like macrophages (THP-I + TGF-β1 condition)[110]. Imaging of the cells from the 4 different conditions was acquired in a Zeiss Primovert inverted microscope with a Zeiss Axiocam ERc s camera, at 72h from the start of the protocol.

3.5 Flow cytometry analysis

After differentiation and polarization of THP-I monocytes, cells from all conditions were removed from the incubator and washed with Dulbecco's phosphate-buffered saline (DPBS) 1X (Gibco; Life Technologies). Detachment of adherent cells was performed by scrapping for the THP-I+PMA, THP-I+LPS and IFN-y and THP-I+TGF-β1 conditions. Centrifugation followed at 277 g for 4 min. Cells from all conditions were then fixed with a Fixing solution 4X (1 volume Fixation/Permeabilization concentrate + 3 volumes Fixation/Permeabilization diluent) (eBioscience™) and incubated at 4°C for 20 min. Cells were then washed with FACS solution (DPBS 1X + 2% FBS). A blocking step was performed with a human Fc receptor binding inhibitor (1:50 in FACS solution) (Invitrogen™) and cells were incubated at 4°C for 10 min. Fluorochrome-tagged monoclonal antibodies were added (1:100 in FACS solution + Fc inhibitor) for the confirmation of the specific phenotypes as followed: against CD14 (PerCP-Cy5.5) for the THP-I control phenotype, against CD16 (PE) for the M0-like phenotype, against CD80

(PE/APC) for the M1-like phenotype and against CD206 (PE-Cy5/eFluor 450) for the M2-like phenotype. Cells were then incubated at 4°C for 40 min. Upon labelling, cells were washed and resuspended in FACS solution and analyzed by flow cytometry.

The initial experiments were performed with monoclonal antibodies targeting TNF-α and IL-10, for the identification of M1-like and M2-like macrophages, respectively. This protocol involved an additional permeabilization step of the cells, after detachment and fixing, attained with a permeabilization buffer 10X (eBioscience™) (1:10 in water) (data not shown).

All data was acquired using the BD LSRFortessa™ cell analyzer (BD Biosciences) with the FACSDiva 6.2 software and later analyzed in the FlowJo™ X 10.0.7r2 software.

3.6 Live-cell staining

THP-I monocytes and THP-I-derived macrophages (M0-, M1- and M2-like) were removed from the incubator and washed with DPBS 1X. Detachment of M0-, M1- and M2-like macrophages was performed by scrapping. Live-cell staining was performed with Dil (Vybrant™; Molecular Probes, Life Technologies, 4 μL/mL in DPBS 1X) for 10 min at 37 °C followed by 15 min on ice in darkness. After centrifugation at 277 g for 4 min, the cell pellet was resuspended in supplemented RPMI1640 medium, and cells were counted on the hemocytometer and included in co-culture for 3D spheroids (3.8.1.).

3.7 P1CP fragment

Recombinant (r) P1CP was supplied by a collaborator of CureBio (KR). rP1CP was produced and purified as described by Seo W.-Y *et al* and it demonstrated high quality and purity[111].

3.8 Analysis of the effect of P1CP *in vitro*

3.8.1 Spheroid formation

In order to produce homo- and heterospheroids, spheroid formation solution was obtained by combining 1 part of 6 mg/ml of methylcellulose solution with 3 parts of high glucose supplemented DMEM, and mitomycin C (1 μg/mL) (Merck Life Sciences) to inhibit cell proliferation. Cancer cells were then resuspended in this solution, alone (homospheroid) or together with THP-I cells or M0-, M1- and M2-like macrophages

(heterospheroids), considering that each homospheroid is composed of 300 cancer cells and each heterospheroid is composed of 300 cancer cells + 700 monocytes/monocyte-derived macrophages. The resulting solution containing cells was plated in a non-adherent round-bottom 384-well microplate (Corning®) at a final volume of 30µL per well. The plate was then placed in an incubator, with a humidified atmosphere containing 5% CO_2 at 37°C, for 72h to allow formation of a single spheroid per well.

3.8.2 Invasion assay of homo- and heterospheroids

The spheroid solution was removed from each well and the spheroid was embedded in a gelatinous matrix mixture consisting of 2 mg/mL of human collagen (StemCell Technologies Inc) and mitomycin C (1 µg/mL). To study the effect of P1CP in invasion of BC cells, 20µg/mL of this fragment was added to the mixture. NaOH was also added to the gel in order to adjust to the correct pH, as in basic conditions collagen monomers nucleate to form thicker collagen fibers, which gelifies the mixture.

After a 1h incubation for solidification at 37°C and 5% CO_2, imaging of the spheroids was performed by fluorescence microscopy in a Zeiss LSM710 confocal microscope. Considering 4 time points of invasion, 0h, 24h, 48h and 72h, different optical cross-sections of the spheroid were captured at different optical planes of a z-stack.

Imagens were then analyzed by counting the number of invading cancer cells using the FIJI/ImageJ software. Invasive cells were considered to be the ones present in the invasive area which is established as the area between the inner perimeter, spheroid border (at time 0h), and the outer perimeter, furthest invaded cell.

3.9 Animal care and handling

Zebrafish (*Danio rerio*) were provided by the fish facility of Instituto de Medicina Molecular (iMM) where they were handled and maintained according to the standard protocols of the European Animal Welfare Legislation, Directive 2010/63/EU (European Commission, 2016), following the Federation of European Laboratory Animal Science Associations (FELASA) guidelines and recommendations. The experimental approach involving this model was approved by ORBEA (Órgão de Bem-Estar e Ética Animal/Animal Welfare and Ethics Body) and DGAV (Direção Geral de Alimentação e Veterinária/Directorate General for Food and Veterinary). All the procedures in this study

were made in early life forms of development with zebrafish embryos below 120 hours post-fertilization (hpf) that do not yet show the ability to feed themselves and are, therefore, considered unprotected under the Directive 2010/63/EU. Tg(mpeg:mCherry;tnf-α:GFP); Tg(mpeg:LRLG)[112] and wild-type AB lines were used according to the aim of each experiment.

3.10 Assessment of the effect of P1CP treatment *in vivo*

3.10.1 Cell preparation for zebrafish xenografts injection

BC cells, GFP-expressing MDA-MB-231, MDA-MB-231 BrM and MDA-MB-231 BO2 were grown in 75 cm^2 flasks until 80% confluency was observed and then washed with DPBS 1X. Detachment was performed with 2 mL of trypsin/EDTA (Gibco) for 5 min at 37ºC, and cells were resuspended in supplemented DMEM for counting.

A $5x10^5$/µl cell concentration of viable cells for injection in zebrafish larvae was obtained by counting on the hemocytometer.

3.10.2 P1CP treatment of zebrafish xenografts

P1CP treatment was performed in the cell preparation step for zebrafish larvae microinjection. The fragment was added to the final mixture, after detachment and counting of BC cells, at a final concentration of 50 µg/mL.

3.10.3 Zebrafish xenografts injection

Approximately 500-1000 BC cells, MDA-MB-231, MDA-MB-231 BrM and MDA-MB-231 BO2 prepared in 3.10.1. were injected into the perivitelline space (PVS) of 1X Tricaine (Sigma-Aldrich) anesthetized 48h hpf larvae. Microinjection was performed under a scope (Leica S8 APO) using borosilicate glass microcapillaries attached to a microinjector (World Precision Instruments, Pneumatic Pico pump PV820) coupled with a micromanipulator (Narishige MN-153). After injection, zebrafish xenografts were transferred to E3 medium and incubated at 34°C (temperature that allows growth of human cancer cell lines not compromising zebrafish larvae development) until the end of experiments. At 24h post-injection (hpi), zebrafish xenografts were screened to verify the

presence or absence of tumoral mass. Non-injected zebrafish larvae, and xenografts with cells in the yolk sac or cellular debris were discarded.

Three days after injection zebrafish xenografts were again screened for the presence or absence of tumoral mass to determine the engraftment rate. Univariate analysis was performed considering all the successfully injected zebrafish xenografts obtained in every experiment.

3.10.4 Imaging processing and analysis of zebrafish xenografts

3.10.4.1 Macrophage recruitment and tumor area progression analysis

At 24hpi and 72hpi, zebrafish xenografts were removed from the incubator for the analysis of macrophage recruitment to the tumor and tumor area progression. Xenografts were firstly anesthetized with tricaine 1X and then mounted between a slide and a coverslip. This process involved placing the xenograft in a drop of tricaine 1X solution on top of the slide and at the center of a platform formed by high vacuum grease (Dow corning). The latter allowed enough separation between the slide and the coverslip on top to keep the larvae motionless without compromising its' integrity.

All images were obtained through fluorescence microscopy in a Zeiss LSM710 confocal microscope, with the z-stack function, normally applying a 10 μm interval between slices. Processing and analysis of the generated images was later performed using the FIJI/ImageJ software.

Macrophage recruitment was quantified through the assessment of the total area of the tumor occupied by macrophages (expressing mCherry) according to the formula below. Total tumor and macrophage areas were measured with the ImageJ software after the sum of all slices of the tumor.

$$Total\ area\ infiltrated\ by\ macrophages\ (\%) = \frac{total\ macrophage\ area}{total\ tumor\ area} \times 100$$

Total tumor areas, at 24hpi and 72hpi, were also calculated for the analysis of tumor area progression upon P1CP treatment.

3.10.4.2 Metastasis formation analysis

At 24hpi and 72hpi, xenografts were removed from the incubator for the analysis of metastasis formation in the head (hindbrain + eye) and in the tail of the zebrafish. Xenografts were anesthetized with tricaine 1X and placed on top of a slide for imaging (as described in 3.10.4.1.).

All images were obtained through fluorescence microscopy in a Zeiss Axio Zoom. V16. stereo microscope. The absolute number of cells composing the micrometastasis present in the head and tail of the zebrafish xenograft were quantified with the ImageJ software cell counter plugin.

3.11 Statistical analysis

Statistical analysis was performed using the GraphPad Prism software version 8. For all statistical analysis, an unpaired *t*-test was applied between two groups in which the *P*-value (*p*) results from a two-tailed test with a confidence interval of 95%, except for the data presented in figure 4.5. (Engraftment analysis) in which Fisher's exact test was applied instead, returning an exact P-value. Statistical differences were considered significant whenever $p < 0.05$ and statistical output was represented by stars as follows: non-significant (ns) when $p > 0.05$; *$p \leq 0.05$; **$p \leq 0.01$; ***$p \leq 0.001$; ****$p \leq 0.0001$. In general, graphs present the results as average (AVG) ± standard error of the mean (SEM) with the exception of figure 4.5. (Engraftment analysis) in which data is represented in the graph as absolute numbers.

4 Results

For the experiments in this project, several human BC cell lines and a human monocytic cell line were selected. The MDA-MB-231 cell line is an epithelial human BC cell line obtained from a patient with a metastatic mammary adenocarcinoma[113]. It is an extremely aggressive, invasive, and poorly differentiated triple-negative BC cell line since it lacks both the estrogen and the progesterone receptors, as well as the HER2 receptor[114,115]. MDA-MB-231 BO2 and MDA-MB-231 BrM cell lines were established after inoculation of MDA-MD-231 cells in mice and present tropism to the bone and brain tissues, respectively[108,109]. Accordingly, the MDA-MB-231 BO2 subclone is a product of the cell culture of metastatic bone specimens generated[108] after MDA-MB-231 inoculation while the MDA-MB-231 BrM subclone was generated from metastasis formed in the brain[109].

4.1 Macrophage stimulation and polarization *in vitro*

As mentioned previously, TAMs present in the TME have been described as an heterogenous population with several sets of markers and subpopulations identified. These subpopulations include 2 types of polarization - M1, which corresponds to a more pro-inflammatory and anti-tumoral phenotype, and M2, which in contrast is associated with an anti-inflammatory and pro-tumoral phenotype. Furthermore, an additional subset in M0 represents the non-activated/unpolarized macrophages that derive from the stimulation and subsequent differentiation of monocytes prior to polarization[116].

To obtain the different subsets of macrophages to be included in the experiments conducted *in vitro*, we performed stimulation and polarization of THP-I cells, a human monocytic cell line. M0-, M1- and M2-like macrophages were generated by *in vitro* stimulation of THP-I monocytes with PMA, LPS + IFN-γ and TGF-β1, respectively. After stimulation, morphological changes denoting phenotypic alterations could be observed between the monocytes and the 3 subsets of monocyte-derived macrophages (figure 4.1A). The polarization status of the different populations was determined and confirmed through flow cytometry analysis of specific markers which upregulation characterizes and identifies the different subsets of macrophages: CD14 (M0-like macrophages), CD80 (M1-like macrophages) and CD206 (M2-like macrophages). Indeed, an increase in expression of CD14, CD80 and CD206 was depicted in monocytes

stimulated by PMA, LPS + IFN-γ and TGF-β1, respectively, confirming the polarization states of M0-, M1- and M2-like macrophages (figure 4.1B).

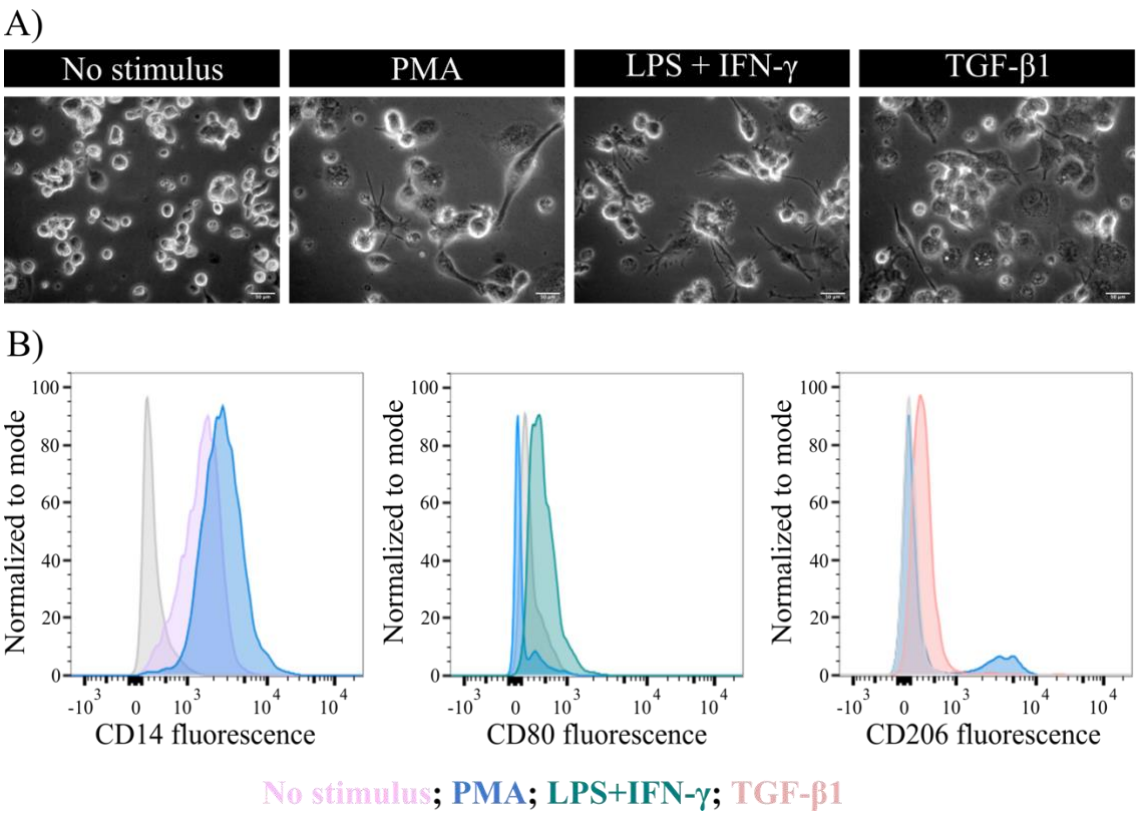

Figure 4.1. Macrophage stimulation and polarization of THP-I cells *in vitro* leads to differential phenotypical changes and expression of specific cell-surface markers. M0-like macrophages were generated by stimulation with PMA. M1- and M2-like macrophages were obtained after polarization with LPS + IFN-γ and TGF-β1, respectively. **A)** Representative microscope images of THP-I cells 72h after stimulation (PMA) and 48h after polarization (LPS + IFN-γ and TGF-β1) acquired in a Zeiss Primovert inverted microscope. **B)** Flow cytometry quantification of CD14-, CD80- and CD206-positive macrophages after stimulation and polarization of THP-I monocytes. Scale bars: 50µm

4.2 P1CP generally increases breast cancer cell invasion in *in vitro* 3D models

Recently, in our lab, P1CP was shown to affect BC cell proliferation in 2D and 3D *in vitro* models. Moreover, a Boyden chamber assay revealed a chemotactic potential of P1CP to attract monocytes, hinting an interaction with the innate immune system (unpublished data).

To further explore the dynamics between P1CP and monocytes/monocyte-derived macrophages in the TME, as well as the possible implications of this interaction in the invasive potential of BC cells, we formed 3D tumor spheroids of BC cells co-cultured with monocytes and monocyte-derived macrophages. After spheroid formation, for the

analysis of BC cell invasion in the presence of P1CP, the latter was added to the spheroids together with a gelatinous matrix mixture of human collagen and mitomycin C, an anti-proliferative drug, ensuring that all observed invaded cells result from their invasive ability and not of cancer cell proliferation. Accordingly, for the 3 selected BC cell lines, MDA-MB-231, MDA-MB-231 BrM and MDA-MB-231 BO2, 10 conditions were tested in parallel for each cell line – P1CP-treated homospheroids and heterospheroids of BC cells with THP-I, M0-, M1- and M2-like macrophages vs matching control of non-treated homospheroids and heterospheroids. After a 1h incubation period for solidification, imaging of the spheroids by confocal microscopy was conducted, considering 4 times points of invasion: 0h, 24h, 48h and 72h.

4.2.1 P1CP treatment of MDA-MB-231 spheroids

For the MDA-MB-231 cell line, in homospheroids, treatment with P1CP directly affected their invasive potential leading to an increased number of invasive cancer cells visible at the 48h time point (p=0.0904) that became significant at 72h (p=0.0248) (figure 4.2B). When comparing treated and non-treated heterospheroids of BC cells with monocytic cells, our results show that P1CP did not lead to a significant increase in invasive ability in any of the time points (24h, p=0.9409; 48h, p=0.1280; 72h, p=0.1055), however a clear tendency can be observed regarding an increase in the number of invasive cells at 48h and 72h (figure 4.2C). Interestingly, the presence of THP-I cells alone did not seem to have an effect in the invasive ability of MDA-MB-231 cells, as shown by the direct comparison between homospheroids and heterospheroids with THP-I cells in absence of P1CP (figure 4.2C).

Concerning the heterospheroids formed with M0-like macrophages, and similar to what was observed in the THP-I heterospheroids, treatment with P1CP did not cause a significant increase in the number of invasive cells in any time point (24h, p=0.5941; 48h, p=0.4518; 72h, p=0.3334) (figure 4.2D). However, in contrast to monocytes, co-culture with M0-like macrophages led to a significant increase in the number of invasive cells at 24h (p=0.0207) and 48h (p=0.0474) compared to the homospheroids (figure 4.2D).

Regarding the effect of P1CP in the invasive ability of cancer cells in heterospheroids co-cultured with M1-like macrophages, the same result was observed, with P1CP demonstrating a tendency to increase the number of invasive cells, especially at 72h, yet without statistical significance in all times points analyzed (24h, p=0.5747; 48h,

p=0.3572; 72h, *p*=0.1218) (figure 4.2E). Unexpectedly, in the heterospheroids, without P1CP treatment, the presence of M1-like macrophages, known to present an anti-tumoral phenotype, did not decrease the number of invasive cells, when compared to the homospheroids, instead a non-significant increase can be observed at 24h (*p*=0.0728) and 48h (*p*=0.1878) (figure 4.2E).

Finally, in the heterospheroids with M2-like macrophages, our results illustrate that the number of invasive cells is not affected by treatment with P1CP at any time point (figure 4.2F). As expected, regardless of the presence of P1CP, when comparing homospheroids with heterospheroids, M2-like macrophages significantly increased cancer cell invasiveness at all time points analyzed (24h, *p*=0.0032; 48h, *p*=0.0159; 72h, *p*=0.0436) (figure 4.2F).

Altogether, for the MDA-MB-231 cell line, our data suggests a direct effect of P1CP in the invasive potential of these cancer cells, which increases through time, independent of the presence of monocytes or monocyte-derived macrophages. However, P1CP seemed to also increase, without significance, the invasive ability of BC cells co-cultured with monocytes and M1-like macrophages.

4.2.2 P1CP treatment of MDA-MB-231 BO2 spheroids

Contrary to what was observed for the MDA-MB-231 cell line, P1CP treatment of MDA-MB-231 BO2 cells, had no direct effect in their invasive ability, as shown by the invasion of homospheroids (figure 4.3B). However, in the presence of monocytic cells, in the heterospheroids with THP-I cells, P1CP led to a significant increase in the number of invasive cells at 48h (*p*=0.0190) (figure 4.3C). Importantly, this significant increase was also verified when comparing P1CP-treated heterospheroids with P1CP-treated homospheroids, in the same time point (48h, *p*=0.0153), denoting the specific effect depending on the presence of THP-I cells (figure 4.3C). As it was the case with the MDA-MB-231 cells, the presence of THP-I cells alone, without P1CP, did not alter the invasiveness of MDA-MB-231 BO2 cells (figure 4.3C).

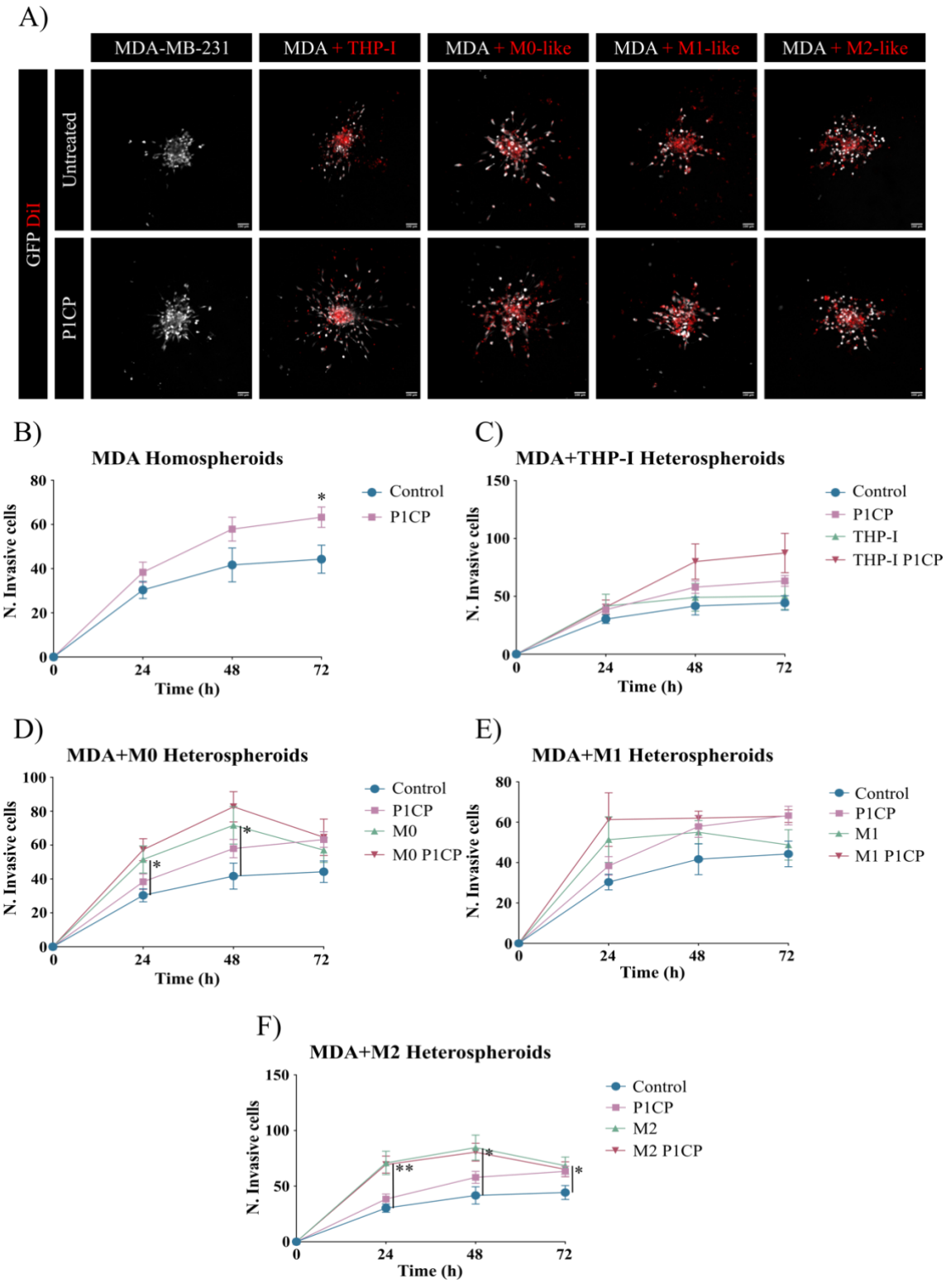

Figure 4.2. Impact of P1CP treatment in the invasion of MDA-MB-231 cells cultured in homospheroids and co-culture in heterospheroids with THP-I cells and THP-I-derived macrophages. A) Representative confocal images of invasion of P1CP-treated MDA-MB-231 homospheroids and heterospheroids with THP-I cells and M0-, M1-, and M2-like macrophages vs non-treated spheroids at 72h. **B)** Quantification of the number of invasive cells in P1CP-treated and non-treated homospheroids at 24h, 48h and 72h of invasion. Error bars represent mean ± SEM. Data were analyzed using an unpaired t-test. **C-F)** Quantification of the number of invasive cells in P1CP-

treated and non-treated heterospheroids of MDA-MB-231cells co-cultured with THP-I cells and M0-, M1-, and M2-like macrophages at 24h, 48h and 72h of invasion. Error bars represent mean ± SEM from at least 3 independent experiments. All data were analyzed using an unpaired *t*-test. Scale bars: 100μm.

As for the heterospheroids with M0-like macrophages, the number of MDA-MB-231 BO2 invasive cells did not change in the presence of P1CP. Surprisingly, without P1CP, in heterospheroids, cancer cells actually presented a significant decrease in invasive ability at 24h (p=0.0031) when compared to homospheroids, but this decreased was less obvious throughout time (figure 4.3D).

As expected, when co-cultured with M1-like macrophages, cancer cells significantly decreased their invasive potential in all time points observed (24h, p<0.0001; 48h, p=0.0004; 72h, p=0.0249) (figure 4.3E). Strikingly, treatment of these heterospheroids with P1CP led to a significant increase in the number of invasive cells at 24h (p=0.0032) and 48h (p=0.0084), and a clear tendency to increase at 72h (p=0.0668) (figure 4.3E).

In accordance with the results obtained with the MDA-MB-231 cell line, in the heterospheroids with M2-like macrophages, P1CP was not able to significantly increase the invasive potential of cancer cells at any time point (24h, p=0.1433; 48h, p=0.2819; 72h, p=0.3632) (figure 4.3F). Unexpectedly, in this cell line, co-culture with M2-like macrophages actually led to a significant decrease in the number of invasive cells at 24h (p=0.0062) and 48h (p=0.0230) (figure 4.3F).

These results point to a possible pro-tumoral interaction between P1CP and M1-like macrophages, which resulted in the rescue of the anti-tumoral phenotype observed in the control group, where BC cells presented a significantly smaller number of invasive cells. Moreover, the presence of P1CP also significantly increased BC cell invasion in heterospheroids of THP-I cells. This effect seems to be dependent of the presence of monocytes, as the significance was maintained in the comparison between P1CP-treated heterospheroids and P1CP-treated homospheroids.

4.2.3 P1CP treatment of MDA-MB-231 BrM spheroids

As observed for the MDA-MB-231 BO2 cell line, P1CP treatment of MDA-MB-231 BrM homospheroids did not lead to a significant direct alteration on cancer cell invasive ability (figure 4.4B). In heterospheroids with THP-I cells, P1CP treatment did not significantly alter the number of invasive cells at any time point, still a clear tendency to

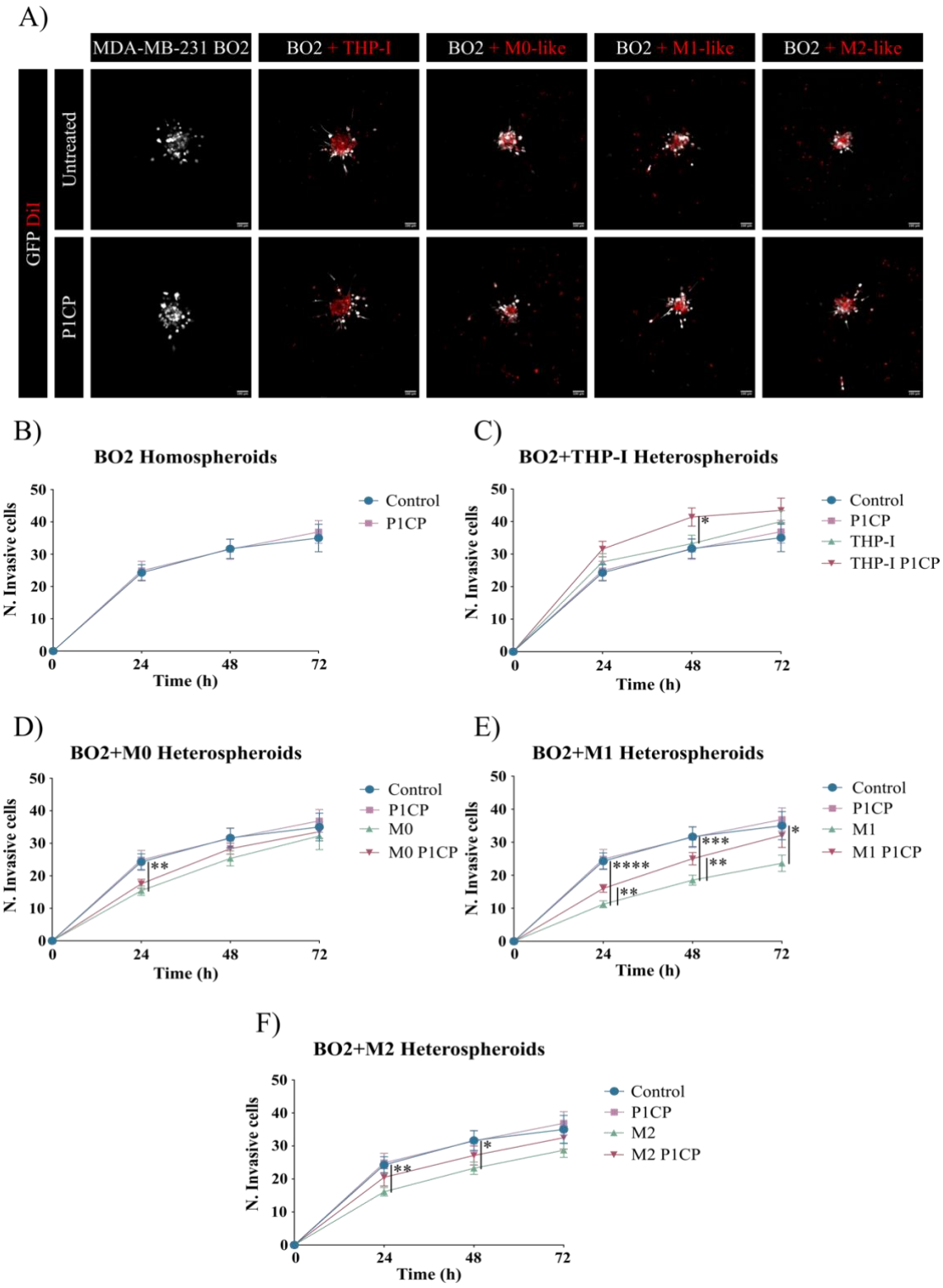

Figure 4.3. Impact of P1CP treatment in the invasion of MDA-MB-231 BO2 cells cultured in homospheroids and co-culture in heterospheroids with THP-I cells and THP-I-derived macrophages. **A)** Representative confocal images of invasion of P1CP-treated MDA-MB-231 BO2 homospheroids and heterospheroids with THP-I cells and M0-, M1-, and M2-like macrophages vs non-treated spheroids at 72h. **B)** Quantification of the number of invasive cells in P1CP-treated and non-treated homospheroids at 24h, 48h and 72h of invasion. Error bars represent mean ± SEM. Data were analyzed using an unpaired t-test. **C-F)** Quantification of the number of invasive cells in P1CP-treated and non-treated heterospheroids of

MDA-MB-231 BO2 cells co-cultured with THP-I cells and M0-, M1-, and M2-like macrophages at 24h, 48h and 72h of invasion. Error bars represent mean ± SEM from at least 3 independent experiments. All data were analyzed using an unpaired *t*-test. Scale bars: 100μm.

an increase can be observed in all time points measured (24h, p=0.1203; 48h, p=0.0853; 72h, p=0.0704) (figure 4.4C). The presence of monocytes alone, however, led to a significant increase at 48h (p=0.0110) and 72h (p=0.0071), as demonstrated by the comparison between homospheroids and heterospheroids with THP-I cells (figure 4.4C).

Interestingly, the presence of P1CP in heterospheroids with M0-like macrophages significantly increased the number of invasive cancer cells at 48h (p=0.0229) and 72h (p=0.0097) (figure 4.4D). Moreover, an increase was also observed when comparing P1CP-treated heterospheroids with P1CP-treated homospheroids at the same time points (48h, p=0.0296; 72h, p=0.0017) (figure 4.4D). M0-macrophages did also directly significantly increase the invasive ability of cancer cells at 24h (p=0.0069) and at 72h (p=0.0128), as demonstrated by the direct comparison between heterospheroids and homospheroids (figure 4.4D).

Regarding the heterospheroid co-cultured with M1-like macrophages, P1CP treatment seems to have no effect in the invasive potential of cancer cells at any time point (24h, p=0.9845; 48h, p=0.3322; 72h, p=0.6516) (figure 4.4E). Unexpectedly, as it happened with the MDA-MB-231 cell line, co-culture with M1-like macrophages did not decrease the number of invasive cells. In contrast, a significant increase can be observed at 48h (p=0.0491) and 72h (p=0.0477), but not at 24h (p=0.3098) (figure 4.4E).

Finally, as observed for the other 2 selected BC cell lines, P1CP treatment of heterospheroids with M2-like macrophages had no effect in the invasive ability of cancer cells (figure 4.4F). As expected, co-culture with M2-like macrophages significantly increased the number of invasive cells at 48h (p=0.0221) and 72h (p=0.0013) (figure 4.4F).

Overall, our results mainly demonstrate that P1CP is able to significantly increase the invasive ability of MDA-MB-231 BrM cells when in the presence of M0-like macrophages. As previously seen, the presence of the innate immune cells is essential for the increase in invasiveness observed upon P1CP treatment, as shown by the results obtained when comparing P1CP-treated heterospheroids and P1CP-treated homospheroids.

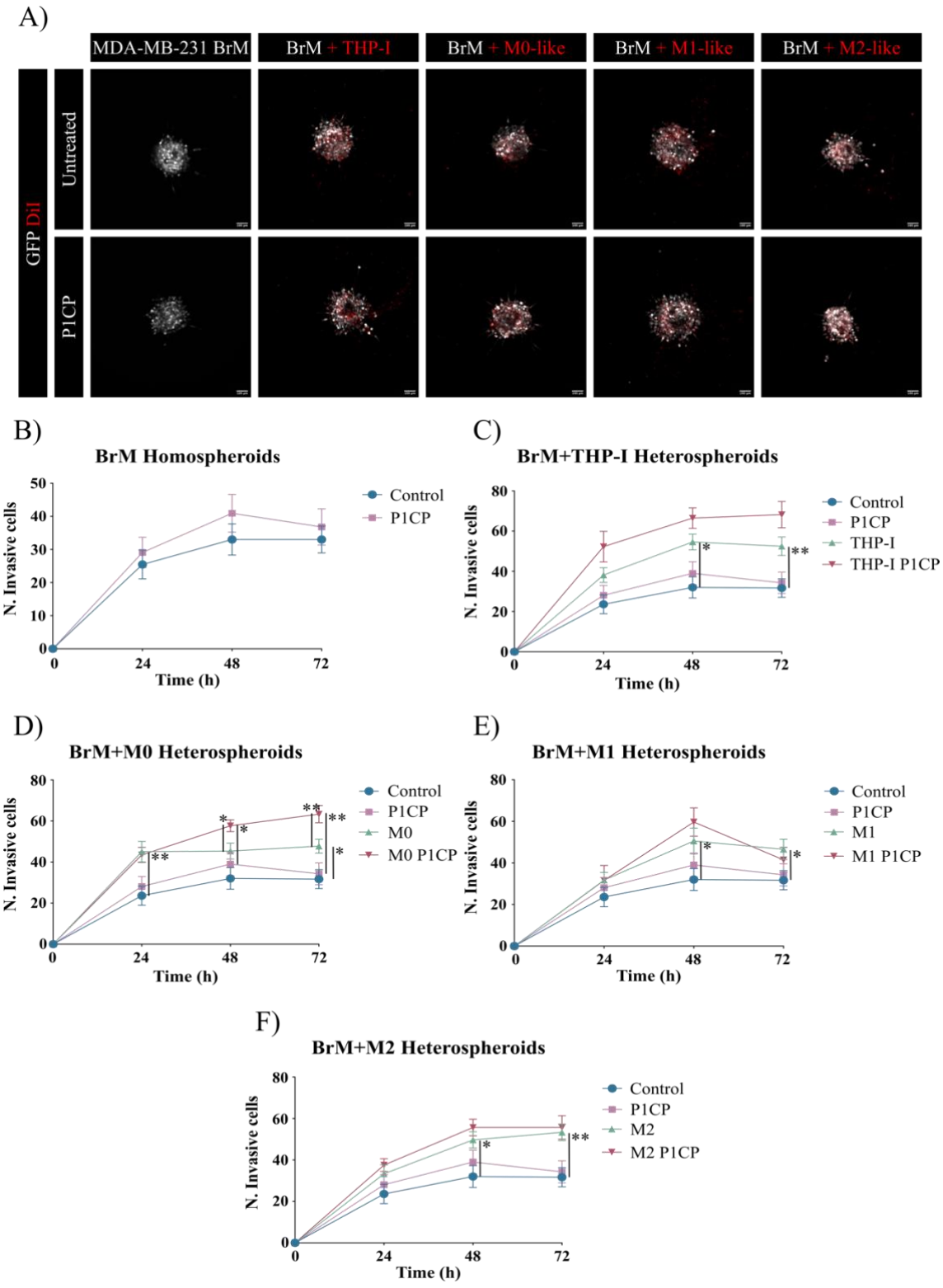

Figure 4.4. Impact of P1CP treatment in the invasion of MDA-MB-231 BrM cells cultured in homospheroids and co-culture in heterospheroids with THP-I cells and THP-I-derived macrophages. **A)** Representative confocal images of invasion of P1CP-treated MDA-MB-231 BrM homospheroids and heterospheroids with THP-I cells and M0-, M1-, and M2-like macrophages vs non-treated spheroids at 72h. **B)** Quantification of the number of invasive cells in P1CP-treated and non-treated homospheroids at 24h, 48h and 72h of invasion. Error bars represent mean ± SEM. Data were analyzed using an unpaired t-test. **C-F)** Quantification of the number of invasive cells in P1CP-treated and non-treated heterospheroids of

MDA-MB-231 BrM cells co-cultured with THP-I cells and M0-, M1-, and M2-like macrophages at 24h, 48h and 72h of invasion. Error bars represent mean ± SEM from at least 3 independent experiments. All data were analyzed using an unpaired *t*-test. Scale bars: 100μm.

4.3 P1CP presents pro-tumoral activity in different breast cancer cell lines *in vivo*

As previously mentioned, the only studies regarding the effect of P1CP in cancer models *in vivo* were performed by Palmieri *et al.* in 2009, but aspects such as metastasis formation and the effect on the innate immune system were not evaluated.

To further explore the pro-tumoral and pro-metastatic activity of P1CP in tumors *in vivo* and study the possible contribution of the innate immune system, specifically of TAMs, we generated zebrafish xenografts through the xenotransplantation of BC cell lines. Untreated and P1CP-treated MDA-MB-231, MDA-MB-231 BO2 and MDA-MB-231 BrM were injected in the PVS of zebrafish larvae at 48 hpf and successfully injected xenografts were selected at 24 hpi. At 24 hpi and 72 hpi, zebrafish xenografts were imaged for the presence of micrometastasis in the head and tail of the larvae, for macrophage recruitment to the tumor, for tumor area progression and for engraftment efficiency.

4.3.1 P1CP increases the engraftment rate of breast cancer cell lines

At 72 hpi, zebrafish xenografts were screened for the presence or absence of tumor for engraftment efficiency analysis of BC cell lines when treated with P1CP. Strikingly, a univariate analysis considering all successfully injected zebrafish xenografts across all experiments, revealed that P1CP treatment led to an overall increase in the engraftment rate of all injected BC cell lines. The proportion of successful engraftment was statistically significant for the MDA-MB-231 (36.8% vs 49.2 %, p=0.0394) (figure 4.5A) and MDA-MB-231 BrM (83.3% vs 96.9%, p=0.0164) (figure 4.5C) cell lines, but not for the MDA-MB-231 BO2 (83.5% vs 91.4%, p=0.1009) cell line (figure 4.5B).

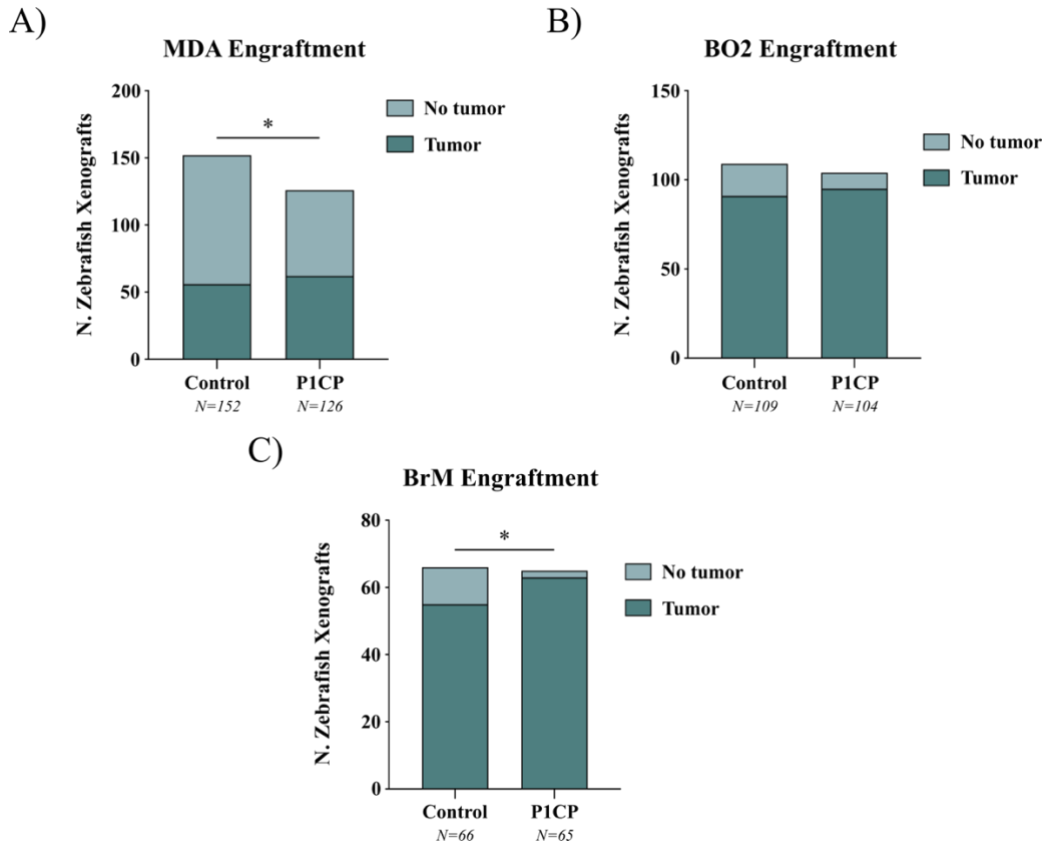

Figure 4.5. P1CP generally increases the engraftment rate of BC tumors in zebrafish xenograft models. Engraftment rate is calculated through the ratio between the number of zebrafish xenografts that retain the tumor at 72 hpi and the total number of xenografts that presented a tumor at 24 hpi and survived until the end of the experiment. BC cell lines, MDA-MB-231, MDA-MB-231 BO2 and MDA-MB-231 BrM, were injected in the PVS of 48 hpf zebrafish embryos. **A)** Engraftment of P1CP-treated vs non-treated MDA-MB-231 tumors. **B)** Engraftment of P1CP-treated vs non-treated MDA-MB-231 BO2 tumors. **C)** Engraftment of P1CP-treated vs non-treated MDA-MB-231BrM tumors. Total number of zebrafish xenografts (*N*) is depicted in the charts. Data were analyzed using a Fisher's exact test.

4.3.2 P1CP treatment differently alters macrophage recruitment in distinct breast cancer cell lines

To investigate if BC cell treatment with P1CP influences macrophage recruitment to the tumor, zebrafish xenografts were generated using the Tg(mpeg:mCherry;tnf-α:GFP); Tg(mpeg:LRLG)[112] transgenic line. This reporter line has the macrophage-expressed gene 1 (MPEG1), a macrophage conserved protein[117], labeled with mCherry, allowing the observation of macrophages in red, with single-cell resolution, under confocal microscopy. Moreover, in this transgenic, TNF-α, a cytokine secreted by M1-like macrophages[118], was labeled with GFP, however the number of GPF-positive zebrafish larvae was extremely low and so the presence of this protein was not considered in this study.

The results obtained show that, in zebrafish xenografts of MDA-MB-231 cells, treatment with P1CP significantly decreased macrophage infiltration in the tumor at 72 hpi (p=0.0036), with a tendency to the same reduction being observed early at 24 hpi (p=0.0937) (figure 4.6A,D). Interestingly, the opposite was observed in zebrafish xenografts of MDA-MB-231 BO2 cells, in which P1CP treatment significantly increased the tumor area infiltrated by macrophages at 24 hpi (p=0.0409) but not at 72 hpi (p=0.2941) (figure 4.6B,E). In the case of the MDA-MB-231 BrM cell line, treatment with P1CP did not lead to a significant alteration in macrophage infiltration in the tumor at any time point (figure 4.6C,F), however a small tendency to increase can be observed at 72 hpi (24h, p=0.4296; 72h, p=0.2098).

These results highlight the different response of distinct BC cell lines to P1CP treatment regarding macrophage recruitment and infiltration in the tumor. Notably, the tumors from the metastatic subclones, MDA-MB-231 BO2 and BrM, presented the same response after treatment, by increasing macrophage infiltration whereas tumors formed by the MDA-MB-231 had a contrasting response.

4.3.3 P1CP treatment increases the metastatic potential of breast cancer cells in vivo

Metastasis can be described as a multistep process, in which 2 main stages can be distinguished. Accordingly, the early steps of metastasis include the ability of tumor cells to move into the interstitial space, by ECM degradation and remodeling, the invasion of nearby tissue and the intravasion into surrounding blood vessels. Later steps include the aptness of tumor cells to survive in circulation, the extravasion from the blood vessels, and colonization at distant sites[119,120].

To further study the effect of P1CP in metastasis formation of BC tumors *in vivo*, including the specific impact on the different steps of the metastatic process, we injected the selected BC cell lines in zebrafish larvae, in the PVS alone (without cells in circulation – no circ) or in the PVS and in circulation (with cells in circulation - circ)[101]. The first group allowed us to investigate the effect of P1CP in the full metastatic cascade, including the first steps of invasion, while the second group will allow analysis on the impact of P1CP only on the steps that proceed the intravasion of blood vessels. We then analyzed, at 24 hpi and 72 hpi, the presence of micrometastasis to the head (hindbrain + eye) and tail of the zebrafish xenograft (figure 4.7).

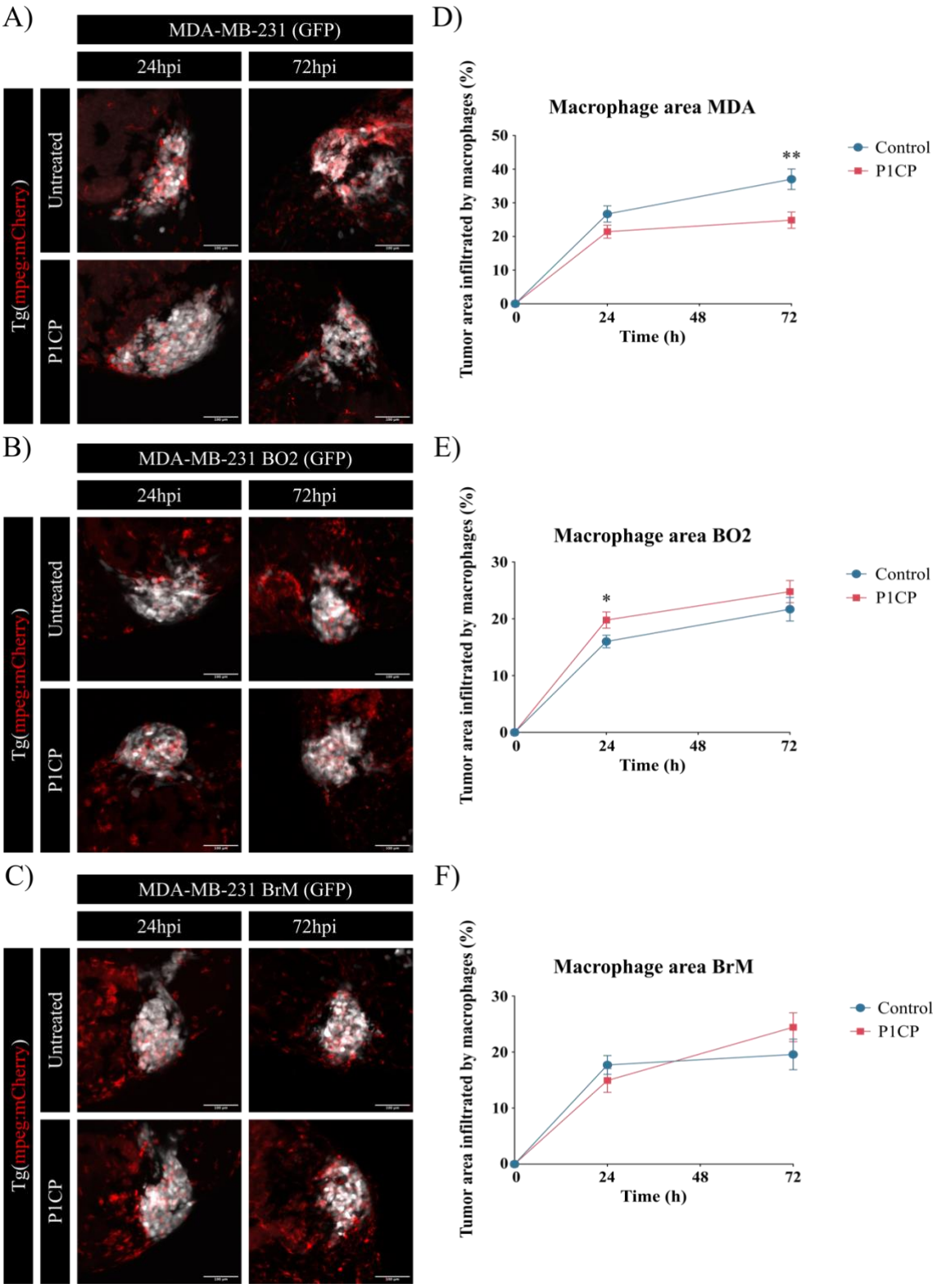

Figure 4.6. Macrophage recruitment of different BC cell lines upon P1CP treatment. A-C) Representative images of confocal microscopy depicting macrophage recruitment (in red) in P1CP-treated vs non-treated MDA-MB-231, MDA-MB-231 BO2 and MDA-MB-231 BrM tumors (in white) from Tg(mpeg:mCherry) zebrafish xenografts, at 24 hpi and 72 hpi. **D-F)** Quantification of tumor area infiltrated by macrophages (total macrophage area/total tumor area x 100) in P1CP-treated vs non-treated MDA-MB-231, MDA-MB-231 BO2 and MDA-MB-231 BrM tumors, at 24 hpi and 72 hpi. Number of xenografts analyzed: in **D)** Control_24hpi N=22, Control_72hpi N=13, P1CP_24hpi N=24, P1CP_72hpi N=17, in **E)**

Control_24hpi N=31, Control_72hpi N=18, P1CP_24hpi N=31, P1CP_72hpi N=26 and in **F)** Control_24hpi N=19, Control_72hpi N=17, P1CP_24hpi N=18, P1CP_72hpi N=23. Error bars represent mean ± SEM. All data were analyzed using an unpaired *t*-test. Scale bars: 100µm.

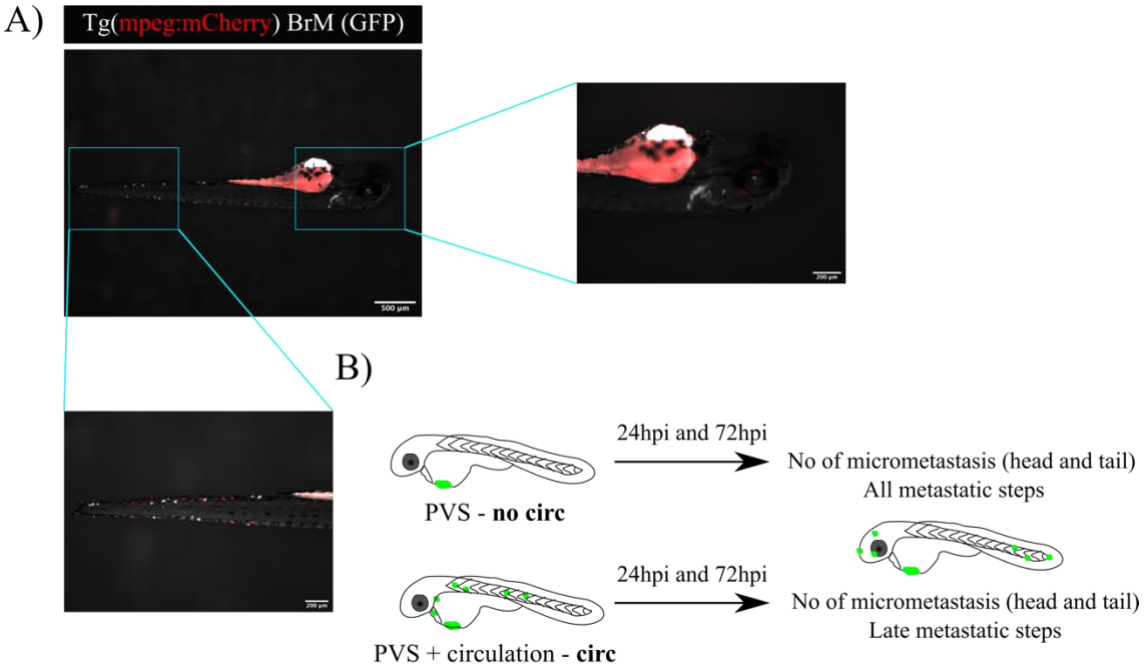

Figure 4.7. Zebrafish xenografts as tools for the study of metastasis formation and invasive ability. A) Representative images of fluorescence microscopy exhibiting MDA-MB-231 BrM micrometastasis formation in the head and tail of the zebrafish xenograft at 24hpi. MDA-MB-231 BrM cells can be denoted in white and the zebrafish macrophages in red. **B)** Schematic representation describing the different sites of injection that allow the study of early vs late metastatic steps in zebrafish xenografts. Scale bars: 500 µm (whole larvae) and 200µm (head and tail).

Our results show that, for the MDA-MB-231 cell line, treatment with P1CP led to an overall significant increase in the number of micrometastasis to the head and to the tail of the zebrafish larvae. Importantly, P1CP seems to have an effect in both early and late stages of the metastatic process. P1CP-treated tumors of MDA-MB-231 cells, injected only in the PVS (no circ), presented a significant increase in the number of micrometastasis to the head, at 24 hpi (p=0.0006) and at 72 hpi (p=0.0089) (figure 4.8A), and also to the tail at both time points (24 hpi, p=0.0029; 72 hpi, p=0.0142) (figure 4.8C). Moreover, when cancer cells were also injected in circulation (circ), similarly P1CP treatment led to a significant increase in metastasis formation in the head, at 24 hpi (p=0.0059) and at 72 hpi (p=0.0071) (figure 4.8B) and in the tail, only at 24 hpi (p=0.0279) (figure 4.8D).

For the MDA-MB-231 BO2 tumors, P1CP treatment presented a minor effect on the formation of micrometastasis in the head and tail of the zebrafish, considering the data

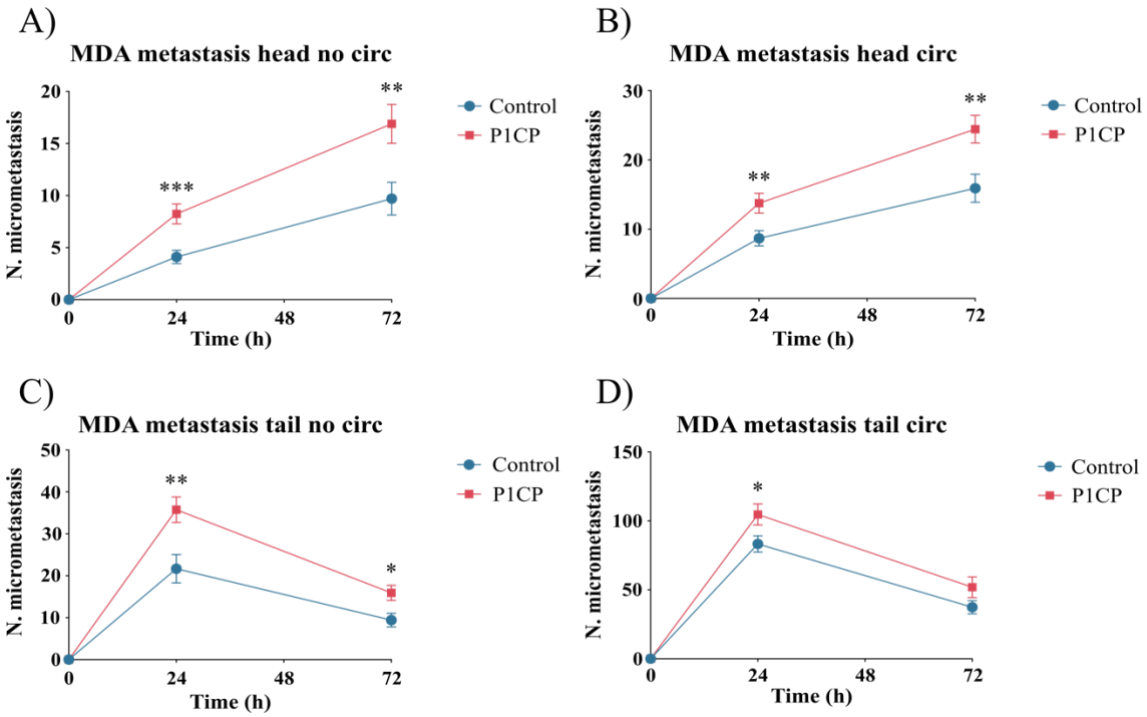

Figure 4.8. P1CP treatment of MDA-MB-231 cells increases micrometastasis formation to the head and tail of the zebrafish xenograft. A-B) Quantification of absolute numbers of micrometastasis in the head of PVS-injected (no circ) and PVS + circulation-injected (circ) zebrafish xenografts with P1CP-treated vs non-treated MDA-MB-231 cells, at 24 hpi and 72 hpi. **C-D)** Quantification of absolute numbers of micrometastasis in the tail of PVS-injected (no circ) and PVS + circulation-injected (circ) zebrafish xenografts with P1CP-treated vs non-treated MDA-MB-231 cells, at 24 hpi and 72 hpi. Number of xenografts analyzed: in **A)** Control_24hpi N=35, Control_72hpi N=20, P1CP_24hpi N=37, P1CP_72hpi N=30, in **B)** Control_24hpi N=44, Control_72hpi N=35, P1CP_24hpi N=28, P1CP_72hpi N=21, in **C)** Control_24hpi N=32, Control_72hpi N=19, P1CP_24hpi N=36, P1CP_72hpi N=28 and **D)** Control_24hpi N=43, Control_72hpi N=34, P1CP_24hpi N=28, P1CP_72hpi N=21. Error bars represent mean ± SEM. All data were analyzed using an unpaired *t*-test.

obtained for the MDA-MB-231 cell line. However, P1CP-treated tumors still presented an overall increase in metastasis formation throughout the experiment. In tumors injected only in the PVS, P1CP treatment caused a significant increase in the number of micrometastasis in the head at 24 hpi (p=0.0161) and a non-significant increase at 72 hpi (p=0.1078) (figure 4.9A). As for the tail, in the same condition, P1CP treatment had no significant effect in micrometastasis formation, still a small tendency can be observed in both time points (24 hpi, p=0.2051; 72 hpi, p=0.1678) (figure 4.9C). Interestingly, when cancer cells were injected also in circulation, P1CP treatment significantly increased the number of metastatic cells only in the tail of the zebrafish larvae at 24 hpi (p=0.0015), with the effect diminishing overtime (figure 4.9D). Analysis of the number of micrometastasis in the head, in the same condition, revealed that P1CP had almost no effect at 24 hpi and a small increase at 72 hpi (p=0.1167), yet not significant (figure 4.9B).

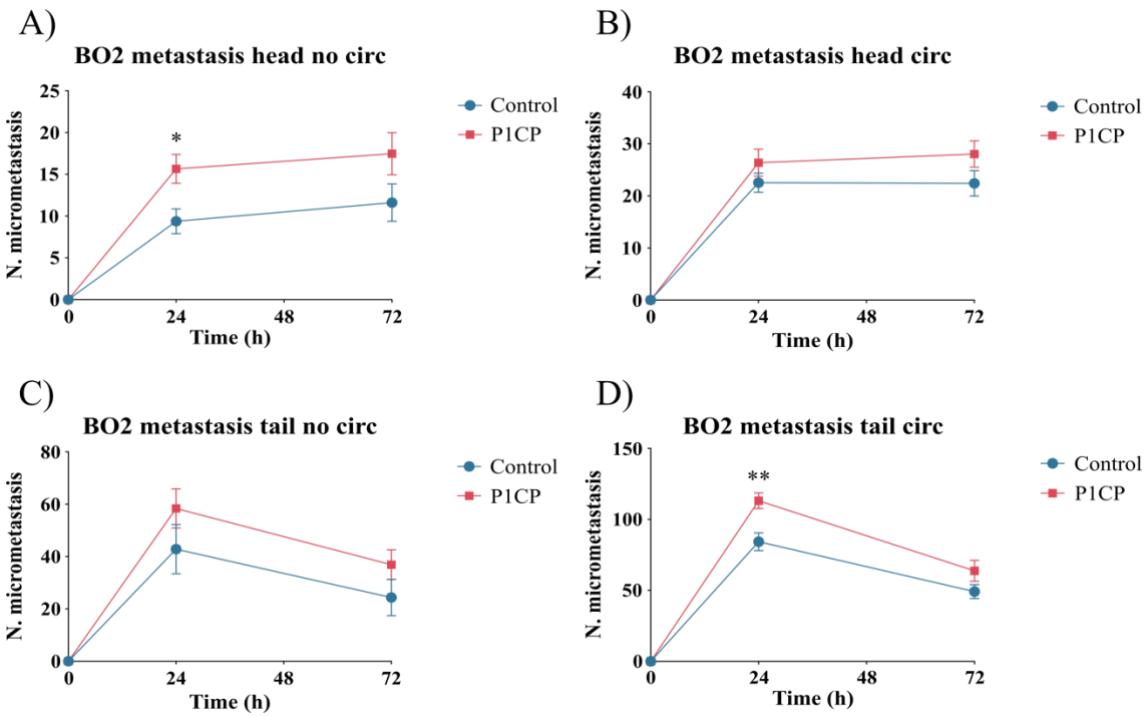

Figure 4.9. P1CP treatment of MDA-MB-231 BO2 cells increases micrometastasis formation to the head and tail of the zebrafish xenograft. A-B) Quantification of absolute numbers of micrometastasis in the head of PVS-injected (no circ) and PVS + circulation-injected (circ) zebrafish xenografts with P1CP-treated vs non-treated MDA-MB-231 BO2 cells, at 24 hpi and 72 hpi. **C-D)** Quantification of absolute numbers of micrometastasis in the tail of PVS-injected (no circ) and PVS + circulation-injected (circ) zebrafish xenografts with P1CP-treated vs non-treated MDA-MB-231 BO2 cells, at 24 hpi and 72 hpi. Number of xenografts analyzed: in **A)** Control_24hpi N=21, Control_72hpi N=18, P1CP_24hpi N=35, P1CP_72hpi N=26, in **B)** Control_24hpi N=26, Control_72hpi N=26, P1CP_24hpi N=24, P1CP_72hpi N=22, in **C)** Control_24hpi N=21, Control_72hpi N=18, P1CP_24hpi N=35, P1CP_72hpi N=26 and **D)** Control_24hpi N=25, Control_72hpi N=27, P1CP_24hpi N=22, P1CP_72hpi N=22. Error bars represent mean ± SEM. All data were analyzed using an unpaired *t*-test.

Concerning the MDA-MB-231 BrM cell line, P1CP treatment of these tumors demonstrated little to no effect on both stages of the metastatic cascade, to the head or tail of the zebrafish larvae throughout the experiment (figure 4.10A-D).

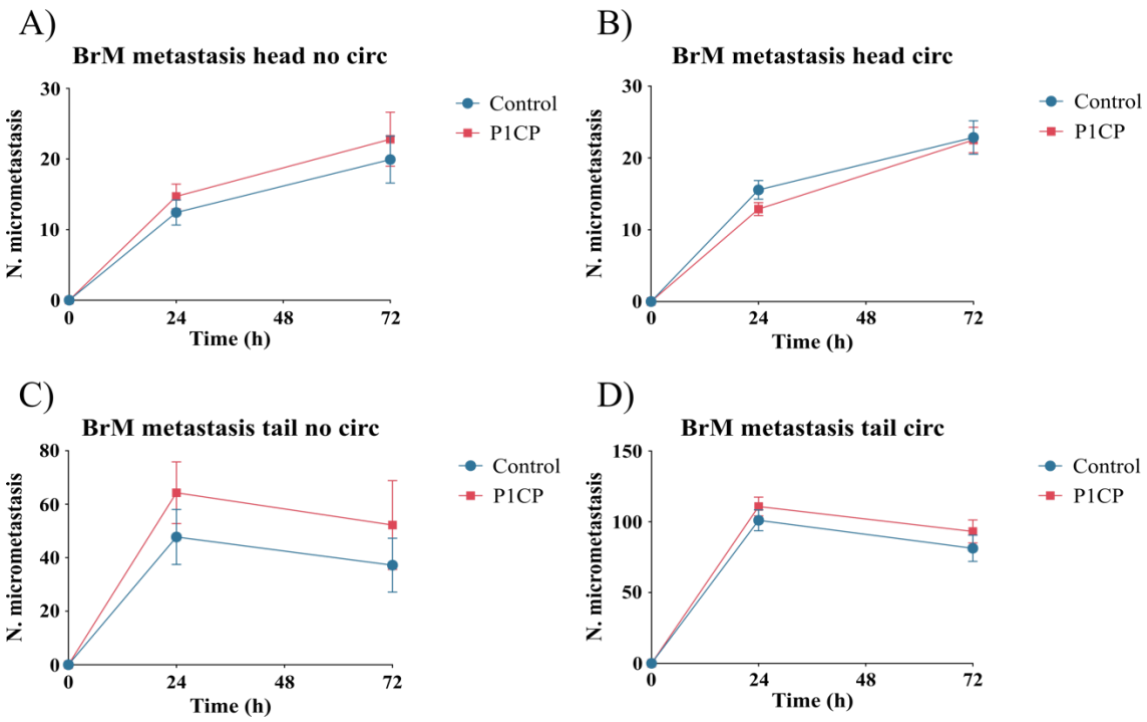

Figure 4.10. P1CP treatment of MDA-MB-231 BrM cells increases micrometastasis formation to the head and tail of the zebrafish xenograft. A-B) Quantification of absolute numbers of micrometastasis in the head of PVS-injected (no circ) and PVS + circulation-injected (circ) zebrafish xenografts with P1CP-treated vs non-treated MDA-MB-231 BrM cells, at 24hpi and 72hpi. **C-D)** Quantification of absolute numbers of micrometastasis in the tail of PVS-injected (no circ) and PVS + circulation-injected (circ) zebrafish xenografts with P1CP-treated vs non-treated MDA-MB-231 BrM cells, at 24hpi and 72hpi. Number of xenografts analyzed: in **A)** Control_24hpi N=27, Control_72hpi N=20, P1CP_24hpi N=18, P1CP_72hpi N=10, in **B)** Control_24hpi N=38, Control_72hpi N=22, P1CP_24hpi N=41, P1CP_72hpi N=24, in **C)** Control_24hpi N=23, Control_72hpi N=19, P1CP_24hpi N=18, P1CP_72hpi N=9 and **D)** Control_24hpi N=34, Control_72hpi N=21, P1CP_24hpi N=35, P1CP_72hpi N=22. Error bars represent mean ± SEM. All data were analyzed using an unpaired *t*-test.

All in all, our data indicates a robust effect of P1CP in promoting the metastatic process, both in the early and late steps of invasion and metastasis formation, mainly in MDA-MB-231 tumors.

4.3.4 Tumor area progression analysis

To further evaluate the pro-tumoral effects of P1CP in BC cells *in vivo*, we analyzed tumor area progression as a measure of tumor growth, by assessing the total area of the tumor at 24 hpi and 72 hpi upon P1CP treatment of the tumors.

Altogether, our results reveal an effect of P1CP treatment mainly in the early phase of tumor formation since significant increases were observed in tumor area at 24 hpi in MDA-MB-231 (p=0.0216) (figure 4.11A) and MDA-MB-231 BrM tumors (p=0.0220)

(figure 4.11C), but not in MDA-MB-231 BO2 tumors (figure 4.11B). This apparent tumor growth-promoting activity of P1CP seems to be compensated in control conditions throughout the experiment, with tumors becoming increasingly similar in area, as demonstrated by the values analyzed at 72 hpi for all BC cell lines (figure 4.11A-C).

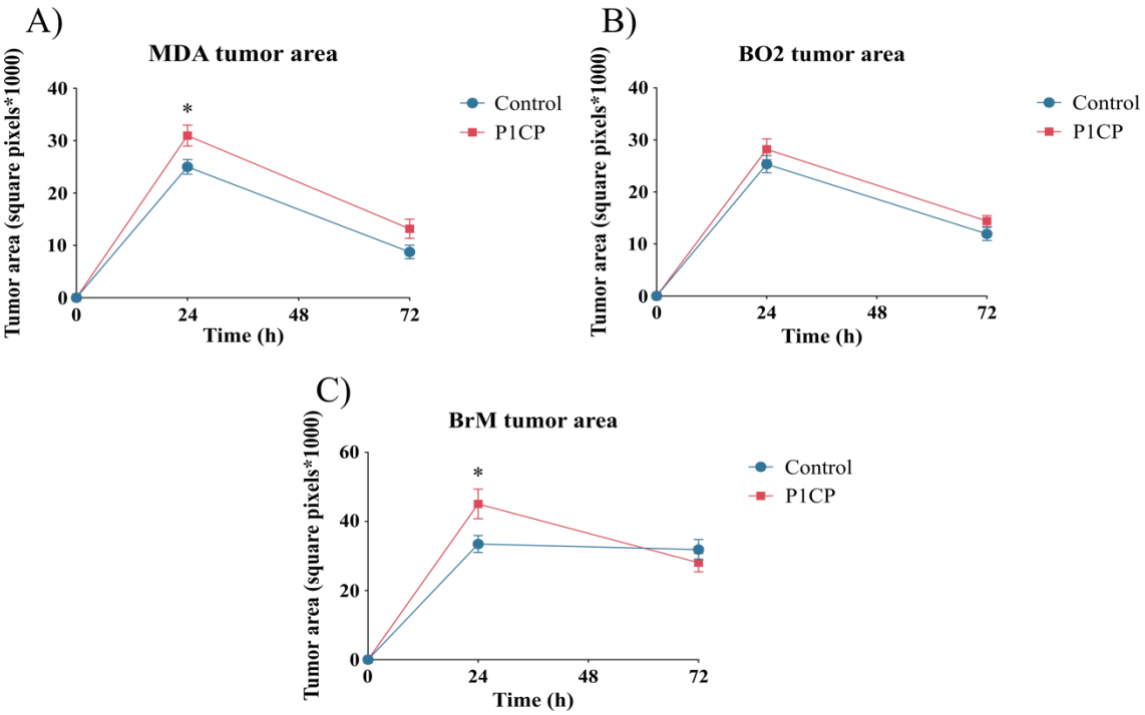

Figure 4.11. Effect of P1CP treatment of BC cells in tumor area progression in zebrafish xenografts. A-C) Tumor area progression curves of P1CP-treated vs non-treated tumors of MDA-MB-231, MDA-MB-231 BO2 and MDA-MB-231 BrM cells, at 24 hpi and 72 hpi. Number of xenografts analyzed: in **A)** Control_24hpi N=23, Control_72hpi N=14, P1CP_24hpi N=26, P1CP_72hpi N=19, in **B)** Control_24hpi N=39, Control_72hpi N=23, P1CP_24hpi N=39, P1CP_72hpi N=36 and in **C)** Control_24hpi N=28, Control_72hpi N=25, P1CP_24hpi N=27, P1CP_72hpi N=29. Error bars represent mean ± SEM. All data were analyzed using an unpaired *t*-test.

5 Discussion

The TME can be defined as a complex structure composed of cancer resident and infiltrating host cells that interact with each other and with the surrounding ECM. In physiological conditions, ECM remodeling and homeostasis, through specific collagen synthesis and degradation, contribute to tissue integrity and function, regulating normal cell behavior[121]. Tumor progression and development relies highly on the dysregulation of ECM remodeling, leading to significant alterations in collagen expression, density, and stiffness[33]. In some cancers, such as BC, during the process of desmoplasia, type I collagen production and deposition is enhanced, while in the invasion process, this protein is degraded by cancer cells[122]. Production of type I collagen originates P1CP and serum levels of P1CP were shown to be robust indicators of bone metastasis in prostate cancer patients[78].

Despite of the strong clinical prognostic value, still little is known about the possible biological effects of P1CP. In this regard, the majority of its described functions were studied by Palmieri *et al*. which identified P1CP has a chemoattractant of endothelial cells and promotor of vascularization *in vitro*[79,80], and by Visigalli *et al*. which confirmed the pro-vascularization ability of P1CP *in vivo*, and, importantly, demonstrated the capability of P1CP to activate pro-migratory signaling cascades and the up-regulation of pro-metastatic genes[29]. Recently, our lab uncovered another function of P1CP has a chemotactic factor to monocytic THP-I cells *in vitro*, establishing a possible interaction with the innate immune system (unpublished data).

In the present study, we further investigated the biological effect of P1CP in BC invasion and metastasis formation and the implication of innate immune cells in these events, specifically monocytes and monocyte-derived macrophages. To achieve this, we applied 2 different models: *in vitro* 3D tumor spheroids and *in vivo* zebrafish larvae xenograft models.

We firstly conducted *in vitro* stimulation and differentiation of THP-I monocytes into M0-like macrophages, a non-activated/unpolarized state, and subsequently polarized them into M1- and M2-like macrophages, known to have anti-tumoral and pro-tumoral phenotypes, respectively. After 24h of stimulation with PMA and 48h after polarization with either LPS + IFN-γ or TGF-β1, we were able to observe major morphological differences between conditions. Monocytes, from the untreated control condition, appeared as small and rounded and most cells were in suspension, whilst monocytes

stimulated with PMA, were larger and presented a more irregular shape, characteristics previously associated with M0-like macrophages[123] and became adherent to the cell culture dish. Moreover, monocytes stimulated with PMA and then polarized with TGF-β1 showed a more flattened, expanded phenotype whilst monocytes polarized with LPS + IFN-γ were smaller and more irregular, developing an elongated spindle-shaped appearance, aspects described as corresponding to M2-, and M1-like macrophages, respectively[123]. Differentiation and polarization of these cells were confirmed by quantification through flow cytometry of specific markers characterizing the different subsets of macrophages.

Tumor 3D homospheroids were formed with BC cell lines, MDA-MB-231, MDA-MB-231 BO2 and MDA-MB-231 BrM. Heterospheroids resulted from the co-culture of BC cells with THP-I monocytes and monocyte-derived M0-, M1-, and M2-like macrophages, generated *in vitro* as described in the previous paragraph. In 3D tumor spheroids of MDA-MB-231 cells, P1CP directly promoted cancer cell invasion, as demonstrated by the significant increase in the number of invasive cells upon treatment of homospheroids. Interestingly, this direct effect in the invasion of BC cells, was not verified for the MDA-MB-231 BO2 and BrM cell lines. This is in accordance with the results obtained by Palmieri *et al.*, which revealed that P1CP induced the migration of MDA-MB-231 cells *in vitro* through the activation of pro-migratory signaling cascades, namely a positive autoregulatory VEGF loop involving the Nrp receptor and a CXCR4/CXCL12 paracrine loop by the overexpression of the CXCR4 receptor[80].

Importantly, treatment with P1CP mainly led to an increase in invasive ability of cancer cells in the presence of monocytes, in all BC cell lines, and M0-like macrophages, particularly in the MDA-MB-231 BrM cell line. Notably, the presence of both immune cells seemed to be essential for the positive effect of P1CP in invasion, since whenever there was a significant increase between P1CP-treated vs untreated heterospheroids, an increase was also observed when comparing P1CP-treated heterospheroids vs P1CP-treated homospheroids. We hypothesize that P1CP may be triggering mechanisms of monocyte differentiation and macrophage polarization favoring more pro-tumoral phenotypes, in a direct or indirect fashion. Furthermore, in heterospheroids of MDA-MB-231 BO2 cells with M1-like macrophages, P1CP demonstrated the ability to rescue the negative impact of the presence of the anti-tumoral immune cells in the invasive ability of BC cells, once more reinforcing a possible pro-tumoral interaction between P1CP and the innate immune cells present in the TME. While there are no studies regarding P1CP,

specifically, as a pro-tumoral agent modulating immune system components, several other collagen-associated matrikines have already been studied in this regard, highlighting the importance of collagen fragments in tumor progression and evasion of the immune system. Accordingly, DGGRYY, a peptide present in the C-terminal telopeptide of the α1 chain of type I collagen, was shown to act as an activator of polymorphonuclear neutrophils[57], whilst the 185-203 peptide of the C-terminal domain of the α3 chain of type IV collagen demonstrated the opposite effect[63]. Moreover, recently, Vijver *et al*. reported that *in vitro* generated MMP-1 and MMP-9 type I collagen fragments were capable of binding and triggering the Leucocyte-Associated Immunoglobin-like Receptor 1 (LAIR-1), an inhibitory receptor present in several immune cell populations[124]. Strikingly, the activation of LAIR-1 by type I collagen fragments was shown to inhibit CD3 signaling and IFN-γ secretion in T cells, promoting immune evasion[124].

Generally, our results demonstrate that P1CP had no impact in BC cell invasion when these cells were co-cultured with M2-like macrophages. This is probably due to the pro-tumoral abilities of these innate immune cells which alone can interact with cancer cells and lead to increased invasion, as previously evidenced[94,125]. Nonetheless, in MDA-MB-231 BO2 co-cultures this was not observed, possibly due to the incapacity of these BC cells to keep the pro-tumoral phenotype of M2-like macrophages. Indeed, macrophages are known to be very plastic cells and depend on different stimuli to keep their polarization status[83]. In spheroids of MDA-MB-231 and MDA-MB-231 BrM cells, co-culture with monocytes and M0-like macrophages also led to a significant increase in invasiveness, which is likely explained by the cancer cells' ability to modulate monocyte differentiation and macrophage polarization into more pro-tumoral phenotypes through the release of specific cytokines[88]. However, in spheroids of the MDA-MB-231 BO2 cell line, the outcome was not the same. In contrast, when co-cultured with M0-like macrophages, a significant decrease could be seen early in the process of invasion, at 24h, that disappeared overtime and co-culture with monocytes had no impact on invasiveness. Therefore, MDA-MB-231 BO2 cells, in this context, may not be capable of inducing monocyte differentiation or macrophage polarization. Moreover, in heterospheroids of MDA-MB-231 BO2 cells with M0-like macrophages, presence of P1CP did not seem to cause an effect in cancer cell invasion contrasting with the results obtained upon P1CP treatment of heterospheroids of the same cell line co-cultured with monocytes, which caused a positive impact on invasive ability that was dependent of the presence of immune

cells. This diversity observed on the impact of P1CP treatment on cancer cell invasion, might related to the presence of different cytokines and soluble factors released by the cancer cells of each individual cell line that can also differ when co-cultured with distinct immune populations. This highlights the need for further studies regarding the direct influence of P1CP in monocyte differentiation and macrophage polarization, the correlation with an increase in invasive ability and how this is impacted by the secretomes of the different co-cultures.

For *in vivo* studies of the pro-tumoral and pro-metastatic activities of P1CP, we generated zebrafish xenografts with the same BC cell lines, MDA-MB-231, MDA-MB-231 BO2 and MDA-MB-231 BrM. Importantly, the presence of P1CP improved the engraftment efficiency of tumors of all 3 BC cell lines, with significant results being observed for the MDA-MB-231 and MDA-MB-231 BrM cell lines. Interestingly, under control conditions (without P1CP treatment), MDA-MB-231 tumors presented a significantly lower engraftment rate when compared to the bone and brain tropic subclones. P1CP treatment also led to a significant decrease in macrophage infiltration of MDA-MB-231 tumors with the opposite effect being observed mainly in tumors of the MDA-MB-231 BO2 cell line. Previous studies regarding engraftment efficiency of BC tumors showed that the downregulation of genes associated with tumor-immune interaction was correlated with a better engraftment rate[126]. Additionally, recent research by Póvoa *et al*., on the process of innate immune evasion in a colorectal cancer zebrafish xenograft model, demonstrated that cancer cell lines with low engraftment rates recruited more neutrophils and macrophages while cancer cell lines that displayed higher engraftment efficiency were capable of polarizing macrophages towards a more pro-tumoral M2-like phenotype[105]. Importantly, neutrophils and macrophages were shown to be essential for tumor clearance and macrophage infiltration was strongly correlated with lower engraftment rates[105]. Accordingly, in our results, the lower engraftment efficiency observed in MDA-MB-231 tumors could be explained by the higher infiltration of macrophages that contribute to its clearance from the host. Therefore, treatment with P1CP may be increasing the engraftment rate of these cells by decreasing macrophage infiltration in the tumor, hinting a possible role of the fragment in immune evasion. Furthermore, MDA-MB-231 BO2 and BrM tumors, which present a higher engraftment efficiency, may be capable of the polarization of macrophages, present in the TME, into the M2-like phenotype. In contrast to what was observed in MDA-MB-231 tumors, P1CP might be increasing the engraftment rate of the bone and brain tropic subclones by

promoting the infiltration of more pro-tumoral macrophages and possibly contributing to the modulation of polarization of these innate immune cells. These results denote a dual effect of P1CP in the recruitment of macrophages which is cell line dependent and most likely due to the different secretome profiles of each BC cell line.

Our results further revealed that P1CP treatment of MDA-MB-231 tumors leads to a significant increase in the number of micrometastasis in the head and tail of the zebrafish xenograft in both conditions of injection: in the PVS + circulation (circ) or just in the PVS (no circ). Hence, in these tumors, P1CP seems to act in early steps of the metastatic process, promoting cancer cell invasion of nearby tissues and intravasion into surrounding blood vessels, but also in late steps contributing for the survival of cancer cells in circulation and establishment of micrometastasis at distant sites. Indeed, Palmieri *et al*. showed that the presence of P1CP in MDA-MB-231 tumors of BalbC/nude mice xenografts, led to an increase in the formation of new vessels, up-regulation of pro metastatic genes (VEGF-A, MMP-9 and CXCR4) and, importantly, down-regulation of the tumor inhibitory gene *RECK*, responsible for the inhibition of MMP-9, MMP-2 and MT1-MMP[29]. These MMPs, mainly the MT1-MMP, were proven to have pivotal roles in the degradation of the basement membrane in BC, allowing tumor cell breakthrough[44]. Accordingly, P1CP may promote the early steps of the metastatic process, namely cancer cell migration and invasion of the surrounding tissue, by inducing the overexpression of MMPs, responsible for the proteolysis of the ECM. P1CP's positive effect on the later steps of the metastatic process can be associated with the promotion of cancer cell survival in circulation, stimulation of the extravasion of tumor cells from the blood vessels or the assurance of the ideal pro-tumoral conditions at the metastatic niche – formation of the pre-metastatic niche. All these processes are strongly dependent on ECM remodeling and degradation by MMPs as well as recruitment of immune populations such as macrophages. Indeed, MMPs secreted by cancer cells were shown to promote the extravasion of CTCs from the blood vessels and facilitate tumor cell infiltration in the pre-metastatic niche[49]. Macrophages were also shown to promote the formation of an ideal pre-metastatic niche and cell survival at the metastatic site by inducing ECM remodeling through the secretion of MMPs, integrins and LOX enzymes[90]. Moreover, in BC, monocyte-derived bone metastasis-associated macrophages were proven critical for bone metastasis outgrowth[94]. Further studies are needed to understand how exactly is P1CP impacting the later stages of the metastatic process, and if it is in any way correlated to MMPs' production and secretion and/or macrophage recruitment and polarization.

Presence of P1CP in MDA-MB-231 BO2 tumors did not lead to the same substantial effect in metastasis formation observed in zebrafish xenografts of the MDA-MB-231 cell line. Still significant differences were observed in the head when larvae were injected in the PVS and in the tail when larvae were injected in circulation. Regarding MDA-MB-231 BrM tumors, P1CP presented almost no effect on metastasis formation. The minor or even lack of effect seen in the bone tropic and mainly in brain tropic tumors compared to MDA-MB-231 tumors, may be due to these cells lines already possessing a pro-metastatic phenotype, possibly capable of ECM remodeling and degradation through specific cytokine and MMPs secretion, as well as immunosuppressive abilities, increasing survival in circulation and at the metastatic site.

Finally, we showed that P1CP treatment of BC tumors did not have a significant long-term impact on tumor growth. Although a small significant increase in tumor area could be seen upon P1CP treatment early at 24hpi in MDA-MB-231 and MDA-MB-231 BrM tumors, this effect was no longer evident at 72hpi. This is in accordance with the previous study performed by Palmieri *et al*. were P1CP treatment of MDA-MB-231 tumors in mice also had no impact on tumor growth[29]. Nonetheless, to confirm these results, ongoing experiments feature the immunostaining of zebrafish xenografts, with P1CP-treated vs untreated tumors, for analysis of proliferation and apoptosis indexes.

6 Conclusion and future perspectives

Overall, the research findings uncovered in this project are promising and confirm a role of the P1CP fragment in cancer cell invasion and metastasis formation of BC tumors, as well as an interaction with monocytes and macrophages present in the TME, fulfilling the main purpose of this thesis.

Monocyte differentiation and macrophage polarization was performed successfully by stimulation *in vitro*, generating 3 different subsets of monocyte-derived macrophages: M0-, M1-, and M2-like macrophages. Spheroids formed by the co-culture of monocytes and monocyte-derived macrophages with BC cell lines, MDA-MB-231, MDA-MB-231 BO2 and MDA-MB-231 BrM, proved to be rapid and quality models to study the impact of P1CP in cancer cell invasion and the interaction with cells from the innate immune system.

Results obtained in *in vitro* 3D spheroid models demonstrated a direct effect of P1CP in cancer cell invasion of MDA-MB-231 cells, in the absence of innate immune cells. In MDA-MB-231 BO2 spheroids, P1CP was able to rescue the anti-invasive effect of M1-like macrophages, and in spheroids of all 3 BC cell lines, presence of P1CP and monocytes significantly increased the number of invasive cells. Moreover, in MDA-MB-231 BrM spheroids, the presence of P1CP and M0-like macrophages also contributed to a significant increase in cancer cell invasiveness. These results demonstrate an overall positive effect of P1CP in BC cell invasion as well as a possible role in monocyte differentiation and macrophage polarization favoring more pro-tumoral phenotypes.

Experiments conducted in *in vivo* zebrafish xenograft models display a possible role of P1CP in immune evasion of BC cells, reflected by an increase in engraftment rate observed in all 3 cell lines and the modulation of macrophage infiltration in the tumor. Furthermore, P1CP treatment of BC tumors resulted in an increase in metastasis formation to the head and tail of the zebrafish larvae, specifically in MDA-MB-231 tumors. This increase was observed when larvae were injected just in the PVS and also in circulation, hinting that P1CP may act on the early and late steps of the metastatic cascade.

To complement this study, it is mandatory to uncover if P1CP has a direct effect in monocyte differentiation and/or macrophage polarization, as it would further explain the results obtained in the heterospheroids and in the zebrafish xenograft models. Accordingly, ongoing experiments feature the stimulation of monocytes and M0-like

macrophages with P1CP and subsequent analysis by flow cytometry of the specific cell surface markers for each macrophage subset (CD14, CD80 and CD206), in order to establish if P1CP has any direct effect on these cells. Moreover, staining of the P1CP-treated vs untreated heterospheroids, targeting the same subset-specific markers, will be performed to investigate possible changes in macrophage polarization status induced by the presence of both P1CP and cancer cells. Further research on a possible macrophage polarization switch induced by P1CP, in the presence of BC cells, could include the quantification of pro-tumoral cytokines and soluble factors secreted by P1CP-treated vs untreated heterospheroids by mass spectrometry. This way, differential secretomes could be established between cell lines, that would better explain the effect of P1CP in the innate immune system.

Since P1CP was already shown to be capable of activating pro-tumoral signaling cascades in MDA-MB-231 cells, culminating in the up and down-regulation of specific cancer-related genes[29,80], and that there all already several collagen receptors described in the literature[127], identification of a P1CP cellular receptor is imperative on the study of its pro-tumoral effects. In this regard, our preliminary results of a proximity ligation assay identified Endo180 as a potential candidate and experiments on-going also address LAIR-1 as another strong possibility. Following identification, receptor-specific compounds blocking the interaction with P1CP and generated KO cells for candidate receptors can be used in the functional studies presented in this thesis, to establish the importance of the P1CP-receptor interaction in these cellular events. Further on, the specific receptor or its interaction with P1CP can be targets for the development of new therapeutic strategies.

Finally, to further explore the effects of P1CP in the metastatic niche and immune evasion and to correlate it with the presence of specific immune populations, co-staining of primary cancer tissue biopsies, of bone and brain metastasis, can be performed targeting P1CP, and markers of specific immune system components previously associated with immune evasion processes and tumor progression, such as M2-like macrophages[90,94] and regulatory T cells[128].

References

1. GLOBOCAN 2020: New Global Cancer Data | UICC.Uicc.org. http://www.uicc.org/news/globocan-2020-new-global-cancer-data. Published 2022. Assessed February 22, 2022

2. Daniel CW, Smith GH. The mammary gland: a model for development. *J Mammary Gland Biol Neoplasia*. 1999;4(1). doi:10.1023/A:1018796301609

3. Winters S, Martin C, Murphy D, Shokar NK. Breast Cancer Epidemiology, Prevention, and Screening. In: *Progress in Molecular Biology and Translational Science*. Vol 151. ; 2017. doi:10.1016/bs.pmbts.2017.07.002

4. Escribà-Agüir V, Rodríguez-Gómez M, Ruiz-Pérez I. Effectiveness of patient-targeted interventions to promote cancer screening among ethnic minorities: A systematic review. *Cancer Epidemiology*. 2016;44. doi:10.1016/j.canep.2016.07.009

5. Kamińska M, Ciszewski T, Łopacka-Szatan K, Miotła P, Starosławska E. Breast cancer risk factors. *Przeglad Menopauzalny*. 2015;14(3). doi:10.5114/pm.2015.54346

6. Perou CM, Sørile T, Eisen MB, et al. Molecular portraits of human breast tumours. *Nature*. 2000;406(6797). doi:10.1038/35021093

7. Sørlie T, Perou CM, Tibshirani R, et al. Gene expression patterns of breast carcinomas distinguish tumor subclasses with clinical implications. *Proc Natl Acad Sci U S A*. 2001;98(19). doi:10.1073/pnas.191367098

8. Yersal O, Barutca S. Biological subtypes of breast cancer: Prognostic and therapeutic implications. *World Journal of Clinical Oncology*. 2014;5(3). doi:10.5306/wjco.v5.i3.412

9. Ovcaricek T, Frkovic SG, Matos E, Mozina B, Borstnar S. Triple negative breast cancer - Prognostic factors and survival. *Radiology and Oncology*. 2011;45(1). doi:10.2478/v10019-010-0054-4

10. Dai X, Li T, Bai Z, et al. Breast cancer intrinsic subtype classification, clinical use and future trends. *American Journal of Cancer Research*. 2015;5(10).

11. Hanahan D, Coussens LM. Accessories to the Crime: Functions of Cells Recruited to the Tumor Microenvironment. *Cancer Cell*. 2012;21(3). doi:10.1016/j.ccr.2012.02.022

12. Hanahan D, Weinberg RA. Hallmarks of cancer: The next generation. *Cell*. 2011;144(5). doi:10.1016/j.cell.2011.02.013

13. Gajewski TF, Schreiber H, Fu YX. Innate and adaptive immune cells in the tumor microenvironment. *Nature Immunology*. 2013;14(10). doi:10.1038/ni.2703

14. Zamarron BF, Chen W. Dual roles of immune cells and their factors in cancer development and progression. *International Journal of Biological Sciences*. 2011;7(5). doi:10.7150/ijbs.7.651

15. Karagiannis GS, Poutahidis T, Erdman SE, Kirsch R, Riddell RH, Diamandis EP. Cancer-associated fibroblasts drive the progression of metastasis through both paracrine and mechanical pressure on cancer tissue. *Molecular Cancer Research*. 2012;10(11). doi:10.1158/1541-7786.MCR-12-0307

16. Chen F, Zhuang X, Lin L, et al. New horizons in tumor microenvironment biology: Challenges and opportunities. *BMC Medicine*. 2015;13(1). doi:10.1186/s12916-015-0278-7

17. Ribeiro Franco PI, Rodrigues AP, de Menezes LB, Pacheco Miguel M. Tumor microenvironment components: Allies of cancer progression. *Pathology Research and Practice*. 2020;216(1). doi:10.1016/j.prp.2019.152729

18. Lu P, Weaver VM, Werb Z. The extracellular matrix: A dynamic niche in cancer progression. *Journal of Cell Biology*. 2012;196(4). doi:10.1083/jcb.201102147

19. Walker C, Mojares E, del Río Hernández A. Role of extracellular matrix in development and cancer progression. *International Journal of Molecular Sciences*. 2018;19(10). doi:10.3390/ijms19103028

20. Cox TR, Erler JT. Remodeling and homeostasis of the extracellular matrix: Implications for fibrotic diseases and cancer. *DMM Disease Models and Mechanisms*. 2011;4(2). doi:10.1242/dmm.004077

21. Egeblad M, Nakasone ES, Werb Z. Tumors as organs: Complex tissues that interface with the entire organism. *Developmental Cell*. 2010;18(6). doi:10.1016/j.devcel.2010.05.012

22. Rozario T, DeSimone DW. The extracellular matrix in development and morphogenesis: A dynamic view. *Developmental Biology*. 2010;341(1). doi:10.1016/j.ydbio.2009.10.026

23. Yue B. Biology of the extracellular matrix: An overview. *Journal of Glaucoma*. 2014;23(8). doi:10.1097/IJG.0000000000000108

24. Frantz C, Stewart KM, Weaver VM. The extracellular matrix at a glance. *Journal of Cell Science*. 2010;123(24). doi:10.1242/jcs.023820

25. Myllyharju J, Kivirikko KI. Collagens, modifying enzymes and their mutations in humans, flies and worms. *Trends in Genetics*. 2004;20(1). doi:10.1016/j.tig.2003.11.004

26. Lu P, Takai K, Weaver VM, Werb Z. Extracellular Matrix degradation and remodeling in development and disease. *Cold Spring Harbor Perspectives in Biology*. 2011;3(12). doi:10.1101/cshperspect.a005058

27. Heneberg P. Paracrine tumor signaling induces transdifferentiation of surrounding fibroblasts. *Critical Reviews in Oncology/Hematology*. 2016;97. doi:10.1016/j.critrevonc.2015.09.008

28. Winkler J, Abisoye-Ogunniyan A, Metcalf KJ, Werb Z. Concepts of extracellular matrix remodelling in tumour progression and metastasis. *Nature Communications*. 2020;11(1). doi:10.1038/s41467-020-18794-x

29. Visigalli D, Palmieri D, Strangio A, et al. The carboxyl terminal trimer of procollagen I induces pro-metastatic changes and vascularization in breast cancer cells xenografts. *BMC Cancer*. 2009;9. doi:10.1186/1471-2407-9-59

30. Kessenbrock K, Plaks V, Werb Z. Matrix Metalloproteinases: Regulators of the Tumor Microenvironment. *Cell*. 2010;141(1). doi:10.1016/j.cell.2010.03.015

31. Huang H. Matrix metalloproteinase-9 (MMP-9) as a cancer biomarker and MMP-9 biosensors: Recent advances. *Sensors (Switzerland)*. 2018;18(10). doi:10.3390/s18103249

32. Li H, Qiu Z, Li F, Wang C. The relationship between MMP-2 and MMP-9 expression levels with breast cancer incidence and prognosis. *Oncology Letters*. 2017;14(5). doi:10.3892/ol.2017.6924

33. Egeblad M, Rasch MG, Weaver VM. Dynamic interplay between the collagen scaffold and tumor evolution. *Current Opinion in Cell Biology*. 2010;22(5). doi:10.1016/j.ceb.2010.08.015

34. Kauppila S, Stenbäck F, Risteli J, Jukkola A, Risteli L. Aberrant type I and type III collagen gene expression in human breast cancer in vivo. *Journal of Pathology*. 1998;186(3). doi:10.1002/(SICI)1096-9896(1998110)186:3<262::AID-PATH191>3.0.CO;2-3

35. Whatcott CJ, Diep CH, Jiang P, et al. Desmoplasia in primary tumors and metastatic lesions of pancreatic cancer. *Clinical Cancer Research*. 2015;21(15). doi:10.1158/1078-0432.CCR-14-1051

36. Barker HE, Chang J, Cox TR, et al. Correction: LOxL2-mediated matrix remodeling in metastasis and mammary gland involution (Cancer Res (2011) 71 (1561–1572) DOI: 10.1158/0008-5472.CAN-10-2868). *Cancer Research*. 2019;79(19). doi:10.1158/0008-5472.CAN-19-2420

37. Erler JT, Bennewith KL, Cox TR, et al. Hypoxia-Induced Lysyl Oxidase Is a Critical Mediator of Bone Marrow Cell Recruitment to Form the Premetastatic Niche. *Cancer Cell*. 2009;15(1). doi:10.1016/j.ccr.2008.11.012

38. Erler JT, Bennewith KL, Nicolau M, et al. Retraction Note: Lysyl oxidase is essential for hypoxia-induced metastasis (Nature, (2006), 440, 7088, (1222-1226), 10.1038/nature04695). *Nature*. 2020;579(7799). doi:10.1038/s41586-020-2112-4

39. Ray A, Slama ZM, Morford RK, Madden SA, Provenzano PP. Enhanced Directional Migration of Cancer Stem Cells in 3D Aligned Collagen Matrices. *Biophysical Journal*. 2017;112(5). doi:10.1016/j.bpj.2017.01.007

40. Conklin MW, Eickhoff JC, Riching KM, et al. Aligned collagen is a prognostic signature for survival in human breast carcinoma. *American Journal of Pathology*. 2011;178(3). doi:10.1016/j.ajpath.2010.11.076

41. Valiathan RR, Marco M, Leitinger B, Kleer CG, Fridman R. Discoidin domain receptor tyrosine kinases: New players in cancer progression. *Cancer and Metastasis Reviews*. 2012;31(1-2). doi:10.1007/s10555-012-9346-z

42. Gao H, Chakraborty G, Zhang Z, et al. Multi-organ Site Metastatic Reactivation Mediated by Non-canonical Discoidin Domain Receptor 1 Signaling. *Cell*. 2016;166(1). doi:10.1016/j.cell.2016.06.009

43. Yuge R, Kitadai Y, Takigawa H, et al. Silencing of Discoidin Domain Receptor-1 (DDR1) Concurrently Inhibits Multiple Steps of Metastasis Cascade in Gastric Cancer. *Translational Oncology*. 2018;11(3). doi:10.1016/j.tranon.2018.02.003

44. Castro-Castro A, Marchesin V, Monteiro P, Lodillinsky C, Rossé C, Chavrier P. Cellular and Molecular Mechanisms of MT1-MMP-Dependent Cancer Cell Invasion. *Annual Review of Cell and Developmental Biology*. 2016;32. doi:10.1146/annurev-cellbio-111315-125227

45. Glentis A, Oertle P, Mariani P, et al. Cancer-associated fibroblasts induce metalloprotease-independent cancer cell invasion of the basement membrane. *Nature Communications*. 2017;8(1). doi:10.1038/s41467-017-00985-8

46. Wolf K, Friedl P. Extracellular matrix determinants of proteolytic and non-proteolytic cell migration. *Trends in Cell Biology*. 2011;21(12). doi:10.1016/j.tcb.2011.09.006

47. Cox TR, Rumney RMH, Schoof EM, et al. The hypoxic cancer secretome induces pre-metastatic bone lesions through lysyl oxidase. *Nature*. 2015;522(7554). doi:10.1038/nature14492

48. Kaplan RN, Riba RD, Zacharoulis S, et al. VEGFR1-positive haematopoietic bone marrow progenitors initiate the pre-metastatic niche. *Nature*. 2005;438(7069). doi:10.1038/nature04186

49. Huang Y, Song N, Ding Y, et al. Pulmonary vascular destabilization in the premetastatic phase facilitates lung metastasis. *Cancer Research*. 2009;69(19). doi:10.1158/0008-5472.CAN-08-4382

50. Oskarsson T, Acharyya S, Zhang XHF, et al. Breast cancer cells produce tenascin C as a metastatic niche component to colonize the lungs. *Nature Medicine*. 2011;17(7). doi:10.1038/nm.2379

51. Malanchi I, Santamaria-Martínez A, Susanto E, et al. Interactions between cancer stem cells and their niche govern metastatic colonization. *Nature*. 2012;481(7379). doi:10.1038/nature10694

52. Pancione M, Remo A, Colantuoni V. Genetic and epigenetic events generate multiple pathways in colorectal cancer progression. *Pathology Research International*. 2012;2012. doi:10.1155/2012/509348

53. Thiery JP, Acloque H, Huang RYJ, Nieto MA. Epithelial-Mesenchymal Transitions in Development and Disease. *Cell*. 2009;139(5). doi:10.1016/j.cell.2009.11.007

54. Gao D, Joshi N, Choi H, et al. Myeloid progenitor cells in the premetastatic lung promote metastases by inducing mesenchymal to epithelial transition. *Cancer Research*. 2012;72(6). doi:10.1158/0008-5472.CAN-11-2905

55. Siméon A, Monier F, Emonard H, et al. Fibroblast-cytokine-extracellular matrix interactions in wound repair. *Curr Top Pathol*. 1999;93. doi:10.1007/978-3-642-58456-5_10

56. Maquart FX, Siméon A, Pasco S, Monboisse JC. Regulation of cell activity by the extracellular matrix: the concept of matrikines. *Journal de la Société de biologie*. 1999;193(4-5). doi:10.1051/jbio/1999193040423

57. Monboisse JC, Bellon G, Randoux A, Dufer J, Borel JP. Activation of human neutrophils by type I collagen. Requirement of two different sequences. *Biochemical Journal*. 1990;270(2). doi:10.1042/bj2700459

58. Maquart FX, Pasco S, Ramont L, Hornebeck W, Monboisse JC. An introduction to matrikines: Extracellular matrix-derived peptides which regulate cell activity - Implication in tumor invasion. *Critical Reviews in Oncology/Hematology*. 2004;49(3). doi:10.1016/j.critrevonc.2003.06.007

59. Zetter BR, Rasmussen N, Brown L. Methods in laboratory investigation: An in vivo assay for chemoattractant activity. *Laboratory Investigation*. 1985;53(3).

60. Lane TF, Iruela-Arispe ML, Johnson RS, Sage EH. SPARC is a source of copper-binding peptides that stimulate angiogenesis. *Journal of Cell Biology*. 1994;125(4). doi:10.1083/jcb.125.4.929

61. Maquart FX, Bellon G, Chaqour B, et al. In vivo stimulation of connective tissue accumulation by the tripeptide- copper complex glycyl-L-histidyl-L-lysine-Cu2+ in rat experimental wounds. *Journal of Clinical Investigation*. 1993;92(5). doi:10.1172/JCI116842

62. Siméon A, Monier F, Emonard H, et al. Expression and activation of matrix metalloproteinases in wounds: Modulation by the tripeptide-copper complex glycyl-L-histidyl-L-lysine- Cu2+. *Journal of Investigative Dermatology*. 1999;112(6). doi:10.1046/j.1523-1747.1999.00606.x

63. Monboisse JC, Garnotel R, Bellon G, et al. The α3 chain of type IV collagen prevents activation of human polymorphonuclear leukocytes. *Journal of Biological Chemistry*. 1994;269(41). doi:10.1016/s0021-9258(18)47275-4

64. Han J, Ohno N, Pasco S, Monboisse JC, Borel JP, Kefalides NA. A cell binding domain from the α3 chain of type IV collagen inhibits proliferation of melanoma cells. *Journal of Biological Chemistry*. 1997;272(33). doi:10.1074/jbc.272.33.20395

65. Pasco S, Han J, Gillery P, et al. A specific sequence of the noncollagenous domain of the α3(IV) chain of type IV collagen inhibits expression and activation of matrix metalloproteinases by tumor cells. *Cancer Research*. 2000;60(2).

66. Maeshima Y, Manfredi M, Reimerli C, et al. Identification of the Anti-angiogenic Site within Vascular Basement Membrane-derived Tumstatin. *Journal of Biological Chemistry*. 2001;276(18). doi:10.1074/jbc.M007764200

67. O'Reilly MS, Boehm T, Shing Y, et al. Endostatin: An endogenous inhibitor of angiogenesis and tumor growth. *Cell*. 1997;88(2). doi:10.1016/S0092-8674(00)81848-6

68. Nissen NI, Karsdal M, Willumsen N. Collagens and Cancer associated fibroblasts in the reactive stroma and its relation to Cancer biology. *Journal of Experimental and Clinical Cancer Research*. 2019;38(1). doi:10.1186/s13046-019-1110-6

69. Suvanto-Luukkonen E, Risteli L, Sundström H, Penttinen J, Kauppila A, Risteli J. Comparison of three serum assays for bone collagen formation during postmenopausal estrogen-progestin therapy. *Clinica Chimica Acta*. 1997;266(2). doi:10.1016/S0009-8981(97)00140-X

70. Francini G, Gonnelli S, Petrioli R, et al. Procollagen Type I Carboxy-Terminal Propeptide as a Marker of Osteoblastic Bone Metastases. *Cancer Epidemiology Biomarkers and Prevention*. 1993;2(2).

71. Scott IC, Blitz IL, Pappano WN, et al. Mammalian BMP-1/Tolloid-related metalloproteinases, including novel family member mammalian Tolloid-like 2, have differential enzymatic activities and distributions of expression relevant to patterning and skeletogenesis. *Developmental Biology*. 1999;213(2). doi:10.1006/dbio.1999.9383

72. Eastell R, Hannon RA. Biochemical markers of bone turnover. In: *Menopause*. ; 2007. doi:10.1016/B978-012369443-0/50034-X

73. Jukkola A, Tähtelä R, Thölix E, et al. Aggressive breast cancer leads to discrepant serum levels of the type I procollagen propeptides PINP and PICP. *Cancer Research*. 1997;57(24).

74. Smedsrod B, Melkko J, Risteli L, Risteli J. Circulating C-terminal propeptide of type I procollagen is cleared mainly via the mannose receptor in liver endothelial cells. *Biochemical Journal*. 1990;271(2). doi:10.1042/bj2710345

75. Taubman MB, Goldberg B, Sherr CJ. Radioimmunoassay for human procollagen. *Science (1979)*. 1974;186(4169). doi:10.1126/science.186.4169.1115

76. Parfitt AM, Simon LS, Villanueva AR, Krane SM. Procollagen type I carboxy-terminal extension peptide in serum as a marker of collagen biosynthesis in bone. Correlation

with iliac bone formation rates and comparison with total alkaline phosphatase. *Journal of Bone and Mineral Research*. 1987;2(5). doi:10.1002/jbmr.5650020510

77. Taubman MB, Kammerman S, Goldberg B. Radioimmunoassay of Procollagen in Serum of Patients with Paget's Disease of Bone. *Proceedings of the Society for Experimental Biology and Medicine*. 1976;152(2). doi:10.3181/00379727-152-39380

78. Nakashima J, Sumitomo M, Miyajima A, et al. The value of serum carboxyterminal propeptide of type 1 procollagen in predicting bone metastases in prostate cancer. *Journal of Urology*. 1997;157(5). doi:10.1016/S0022-5347(01)64847-X

79. Palmieri D, Camardella L, Ulivi V, Guasco G, Manduca P. Trimer carboxyl propeptide of collagen I produced by mature osteoblasts is chemotactic for endothelial cells. *Journal of Biological Chemistry*. 2000;275(42). doi:10.1074/jbc.M002698200

80. Palmieri D, Astigiano S, Barbieri O, et al. Procollagen I COOH-terminal fragment induces VEGF-A and CXCR4 expression in breast carcinoma cells. *Experimental Cell Research*. 2008;314(11-12). doi:10.1016/j.yexcr.2008.04.016

81. Curren Smith EW. Macrophage Polarization and Its Role in Cancer. *Journal of Clinical & Cellular Immunology*. 2015;06(04). doi:10.4172/2155-9899.1000338

82. Janeway's Immunobiology. 9th ed. New York: Garland Science, Taylor & Francis Group; 2017:1-77

83. Wynn TA, Chawla A, Pollard JW. Macrophage biology in development, homeostasis and disease. *Nature*. 2013;496(7446). doi:10.1038/nature12034

84. Galdiero MR, Garlanda C, Jaillon S, Marone G, Mantovani A. Tumor associated macrophages and neutrophils in tumor progression. *Journal of Cellular Physiology*. 2013;228(7). doi:10.1002/jcp.24260

85. Norton SE, Dunn ETJ, McCall JL, Munro F, Kemp RA. Gut macrophage phenotype is dependent on the tumor microenvironment in colorectal cancer. *Clinical and Translational Immunology*. 2016;5(4). doi:10.1038/cti.2016.21

86. Hao NB, Lü MH, Fan YH, Cao YL, Zhang ZR, Yang SM. Macrophages in tumor microenvironments and the progression of tumors. *Clinical and Developmental Immunology*. 2012;2012. doi:10.1155/2012/948098

87. Viola A, Munari F, Sánchez-Rodríguez R, Scolaro T, Castegna A. The metabolic signature of macrophage responses. *Frontiers in Immunology*. 2019;10(JULY). doi:10.3389/fimmu.2019.01462

88. Chanmee T, Ontong P, Konno K, Itano N. Tumor-associated macrophages as major players in the tumor microenvironment. *Cancers (Basel)*. 2014;6(3). doi:10.3390/cancers6031670

89. Scholl SM, Pallud C, Beuvon F, et al. Anti-colony-stimulating factor-1 antibody staining in primary breast adenocarcinomas correlates with marked inflammatory cell infiltrates and prognosis. *J Natl Cancer Inst*. 1994;86(2). doi:10.1093/jnci/86.2.120

90. Lin Y, Xu J, Lan H. Tumor-associated macrophages in tumor metastasis: Biological roles and clinical therapeutic applications. *Journal of Hematology and Oncology*. 2019;12(1). doi:10.1186/s13045-019-0760-3

91. Laoui D, Movahedi K, van Overmeire E, et al. Tumor-associated macrophages in breast cancer: Distinct subsets, distinct functions. *International Journal of Developmental Biology*. 2011;55(7-9). doi:10.1387/ijdb.113371dl

92. Li H, Yang B, Huang J, et al. Cyclooxygenase-2 in tumor-associated macrophages promotes breast cancer cell survival by triggering a positive-feedback loop between macrophages and cancer cells. *Oncotarget*. 2015;6(30). doi:10.18632/oncotarget.4936

93. Maller O, Drain AP, Barrett AS, et al. Tumour-associated macrophages drive stromal cell-dependent collagen crosslinking and stiffening to promote breast cancer aggression. *Nature Materials*. 2021;20(4). doi:10.1038/s41563-020-00849-5

94. Ma RY, Zhang H, Li XF, et al. Monocyte-derived macrophages promote breast cancer bone metastasis outgrowth. *Journal of Experimental Medicine*. 2020;217(11). doi:10.1084/JEM.20191820

95. Costa EC, Moreira AF, de Melo-Diogo D, Gaspar VM, Carvalho MP, Correia IJ. 3D tumor spheroids: an overview on the tools and techniques used for their analysis. *Biotechnology Advances*. 2016;34(8). doi:10.1016/j.biotechadv.2016.11.002

96. Mehta G, Hsiao AY, Ingram M, Luker GD, Takayama S. Opportunities and challenges for use of tumor spheroids as models to test drug delivery and efficacy. *Journal of Controlled Release*. 2012;164(2). doi:10.1016/j.jconrel.2012.04.045

97. Saraiva DP, Matias AT, Braga S, Jacinto A, Cabral MG. Establishment of a 3D Co-culture With MDA-MB-231 Breast Cancer Cell Line and Patient-Derived Immune Cells for Application in the Development of Immunotherapies. *Frontiers in Oncology*. 2020;10. doi:10.3389/fonc.2020.01543

98. Murphy JF. Patient-Derived Xenograft (PDX) Models: An Emerging Platform for Cancer Drug Development and Translational Research. *MOJ Immunology*. 2016;3(4). doi:10.15406/moji.2016.03.00094

99. Chen X, Li Y, Yao T, Jia R. Benefits of Zebrafish Xenograft Models in Cancer Research. *Frontiers in Cell and Developmental Biology*. 2021;9. doi:10.3389/fcell.2021.616551

100. Fior R, Póvoa V, Mendes R v., et al. Single-cell functional and chemosensitive profiling of combinatorial colorectal therapy in zebrafish xenografts. *Proc Natl Acad Sci U S A*. 2017;114(39). doi:10.1073/pnas.1618389114

101. Rebelo de Almeida C, Mendes RV, Pezzarossa A, et al. Zebrafish xenografts as a fast screening platform for bevacizumab cancer therapy. *Communications Biology*. 2020;3(1). doi:10.1038/s42003-020-1015-0

102. Renshaw SA, Trede NS. A model 450 million years in the making: Zebrafish and vertebrate immunity. *DMM Disease Models and Mechanisms*. 2012;5(1). doi:10.1242/dmm.007138

103. Haldi M, Ton C, Seng WL, McGrath P. Human melanoma cells transplanted into zebrafish proliferate, migrate, produce melanin, form masses and stimulate angiogenesis in zebrafish. *Angiogenesis*. 2006;9(3). doi:10.1007/s10456-006-9040-2

104. Marques IJ, Weiss FU, Vlecken DH, et al. Metastatic behaviour of primary human tumours in a zebrafish xenotransplantation model. *BMC Cancer*. 2009;9. doi:10.1186/1471-2407-9-128

105. Póvoa V, Rebelo de Almeida C, Maia-Gil M, et al. Innate immune evasion revealed in a colorectal zebrafish xenograft model. *Nature Communications*. 2021;12(1). doi:10.1038/s41467-021-21421-y

106. Veinotte CJ, Dellaire G, Berman JN. Hooking the big one: The potential of zebrafish xenotransplantation to reform cancer drug screening in the genomic era. *DMM Disease Models and Mechanisms*. 2014;7(7). doi:10.1242/dmm.015784

107. Novoa B, Figueras A. Zebrafish: Model for the study of inflammation and the innate immune response to infectious diseases. *Advances in Experimental Medicine and Biology*. 2012;946. doi:10.1007/978-1-4614-0106-3_15

108. Peyruchaud O, Winding B, Pécheur I, Serre CM, Delmas P, Clézardin P. Early detection of bone metastases in a murine model using fluorescent human breast cancer cells: Application to the use of the bisphosphonate zoledronic acid in the treatment of osteolytic lesions. *Journal of Bone and Mineral Research*. 2001;16(11). doi:10.1359/jbmr.2001.16.11.2027

109. Yoneda T, Williams PJ, Hiraga T, Niewolna M, Nishimura R. A bone-seeking clone exhibits different biological properties from the MDA-MB-231 parental human breast cancer cells and a brain-seeking clone in vivo and in vitro. *Journal of Bone and Mineral Research*. 2001;16(8). doi:10.1359/jbmr.2001.16.8.1486

110. Zhang F, Wang H, Wang X, et al. TGF-β induces M2-like macrophage polarization via SNAILmediated suppression of a pro-inflammatory phenotype. *Oncotarget*. 2016;7(32). doi:10.18632/oncotarget.10561

111. Seo WY, Kim JH, Baek DS, et al. Production of recombinant human procollagen type i C-terminal propeptide and establishment of a sandwich ELISA for quantification. *Scientific Reports*. 2017;7(1). doi:10.1038/s41598-017-16290-9

112. Nguyen-Chi M, Laplace-Builhe B, Travnickova J, et al. Identification of polarized macrophage subsets in zebrafish. *Elife*. 2015;4(JULY 2015). doi:10.7554/eLife.07288

113. Cailleau R, Olivé M, Cruciger QVJ. Long-term human breast carcinoma cell lines of metastatic origin: Preliminary characterization. *In Vitro*. 1978;14(11). doi:10.1007/BF02616120

114. Liu H, Zang C, Fenner MH, Possinger K, Elstner E. PPARγ ligands and ATRA inhibit the invasion of human breast cancer cells in vitro. *Breast Cancer Research and Treatment*. 2003;79(1). doi:10.1023/A:1023366117157

115. Chavez KJ, Garimella S v., Lipkowitz S. Triple negative breast cancer cell lines: One tool in the search for better treatment of triple negative breast cancer. *Breast Disease*. 2010;32(1-2). doi:10.3233/BD-2010-0307

116. Orekhov AN, Orekhova VA, Nikiforov NG, et al. Monocyte differentiation and macrophage polarization. *Vessel Plus*. 2019;3. doi:10.20517/2574-1209.2019.04

117. Benard EL, Racz PI, Rougeot J, et al. Macrophage-expressed perforins Mpeg1 and Mpeg1.2 have an anti-bacterial function in zebrafish. *Journal of Innate Immunity*. 2015;7(2). doi:10.1159/000366103

118. Atri C, Guerfali FZ, Laouini D. Role of human macrophage polarization in inflammation during infectious diseases. *International Journal of Molecular Sciences*. 2018;19(6). doi:10.3390/ijms19061801

119. Nguyen DX, Bos PD, Massagué J. Metastasis: From dissemination to organ-specific colonization. *Nature Reviews Cancer*. 2009;9(4). doi:10.1038/nrc2622

120. Valastyan S, Weinberg RA. Tumor metastasis: Molecular insights and evolving paradigms. *Cell*. 2011;147(2). doi:10.1016/j.cell.2011.09.024

121. Bonnans C, Chou J, Werb Z. Remodelling the extracellular matrix in development and disease. *Nature Reviews Molecular Cell Biology*. 2014;15(12). doi:10.1038/nrm3904

122. Willumsen N, Ali SM, Leitzel K, et al. Collagen fragments quantified in serum as measures of desmoplasia associate with survival outcome in patients with advanced pancreatic cancer. *Scientific Reports*. 2019;9(1). doi:10.1038/s41598-019-56268-3

123. Rostam HM, Reynolds PM, Alexander MR, Gadegaard N, Ghaemmaghami AM. Image based Machine Learning for identification of macrophage subsets. *Scientific Reports*. 2017;7(1). doi:10.1038/s41598-017-03780-z

124. Vijver S v., Singh A, Mommers-Elshof ETAM, et al. Collagen Fragments Produced in Cancer Mediate T Cell Suppression Through Leukocyte-Associated Immunoglobulin-Like Receptor 1. *Frontiers in Immunology*. 2021;12. doi:10.3389/fimmu.2021.733561

125. Vinnakota K, Zhang Y, Selvanesan BC, et al. M2-like macrophages induce colon cancer cell invasion via matrix metalloproteinases. *Journal of Cellular Physiology*. 2017;232(12). doi:10.1002/jcp.25808

126. Moon HG, Oh K, Lee J, et al. Prognostic and functional importance of the engraftment-associated genes in the patient-derived xenograft models of triple-negative breast

cancers. *Breast Cancer Research and Treatment*. 2015;154(1). doi:10.1007/s10549-015-3585-y

127. Boraschi-Diaz I, Wang J, Mort JS, Komarova S v. Collagen type i as a ligand for receptor-mediated signaling. *Frontiers in Physics*. 2017;5(MAY). doi:10.3389/fphy.2017.00012

128. Stenström J, Hedenfalk I, Hagerling C. Regulatory T lymphocyte infiltration in metastatic breast cancer—an independent prognostic factor that changes with tumor progression. *Breast Cancer Research*. 2021;23(1). doi:10.1186/s13058-021-01403-0